1

Rapid #: -4430033

Odyssey IP: 206.107.42.78/ILL

Status	Rapid Code	Branch Name	Start Date
Pending	IQU	CSEL	5/10/2011 1:11:54 PM

CALL #: QE340 G413
LOCATION: IQU :: CSEL :: sper ,sper1

TYPE: Article CC:CCL
JOURNAL TITLE: Australian journal of earth sciences
USER JOURNAL TITLE: Australian journal of earth sciences.
IQU CATALOG TITLE: Australian journal of earth sciences / Geological Society of Australia
ARTICLE TITLE: Age constraints on the geological evolution of the Narryer Gneiss Complex, Western Australia
ARTICLE AUTHOR: Kinny P. D.; J. R. Wijbrans; D. O. Froude; I. S. W
VOLUME: 37
ISSUE: 1
MONTH:
YEAR: 1990
PAGES: 51-69
ISSN: 0812-0099
OCLC #: 11297431
CROSS REFERENCE ID: [TN:231489][ODYSSEY:206.107.42.78/ILL]
VERIFIED:

REQUEST UPDATED TO FILLED

BORROWER: MYG :: Main Library
PATRON: Benjamin Weiss
PATRON ID: bpweiss@mit.edu
PATRON ADDRESS:
PATRON PHONE:
PATRON FAX:
PATRON E-MAIL:
PATRON DEPT:
PATRON STATUS:
PATRON NOTES:

Australian Journal of Earth Sciences (1990) **37**, 51–69

Age constraints on the geological evolution of the Narryer Gneiss Complex, Western Australia

P. D. KINNY, J. R. WIJBRANS,* D. O. FROUDE,† I. S. WILLIAMS AND W. COMPSTON

Research School of Earth Sciences, Australian National University, GPO Box 4, Canberra, ACT 2601, Australia.

Zircon U–Th–Pb and mineral K–Ar and $^{40}Ar/^{39}Ar$ isotopic studies indicate that the maximum deposition age of the Mt Narryer quartzite (which contains detrital zircons up to 4200 Ma old) is 3280 Ma, or by association with other sequences possibly 3100 Ma. This postdates a major episode of high-grade metamorphism, granite emplacement and deformation at 3300 Ma, which affected adjacent gneiss terranes and which previously had been considered to have affected metasediments and basement gneisses alike. Prograde metamorphism of the Narryer metasediments to amphibolite facies evidently took place during a younger event culminating *ca* 2700 Ma, prior to injection of granite sheets *ca* 2650 Ma in age, by which time the present tectonic framework had been assembled.

Key words: $^{40}Ar/^{39}Ar$ dating, Narryer Gneiss Complex, Yilgarn Craton, zircon dating.

INTRODUCTION

Metasedimentary rocks exposed at Mt Narryer in the northwestern corner of the Archaean Yilgarn craton of Western Australia contain detrital zircons that are remnants of the Earth's oldest known crust (Froude *et al* 1983). The sediments lie in tectonic contact with ancient orthogneisses from which original crystallization ages ranging from 3380 to 3730 Ma were determined, using zircon Pb–Pb and U–Pb analyses (Kinny *et al* 1988a). These ages were in agreement with other, less precise, dating methods (de Laeter *et al* 1981, 1985; Fletcher *et al* 1988). From isotopic studies of selected minerals, this paper examines the age of deposition of the metasediments and their relationship to the orthogneisses, and discusses the metamorphic history of the region. These aspects of the geological history are relevant to broader considerations of crustal evolution in the Yilgarn craton because knowledge of the time of deposition may constrain assessments of the time at which crust $\geqslant$4100 Ma in age was still exposed at the Earth's surface, and because it is believed that there are links between the metamorphic history of the ancient gneiss complex and the development of the younger granite–greenstone terranes of the eastern and central Yilgarn (Gee *et al* 1986). In addition to evidence from both sedimentary and igneous zircon suites, the metamorphic history of the region is examined by K–Ar and $^{40}Ar/^{39}Ar$ age spectrum techniques, techniques particularly sensitive to thermal events.

The Narryer Gneiss Complex is the largest of three discrete provinces on the western margin of the Yilgarn craton in which rocks over 3 Ga old have been identified (Myers 1988a). Detailed accounts of the geology in the vicinity of Mt Narryer were given by Myers and Williams (1985) and Myers (1988a). The quartzite in which the extremely old detrital zircons were first found forms part of a prominently exposed deformed sequence of quartzites, meta-conglomerates and minor pelitic gneisses and amphibolites, which are tectonically included in quartzo-feldspathic orthogneisses (Fig. 1). Myers and Williams (1985) distinguished two main generations of orthogneisses at Mt Narryer: the Meeberrie gneiss, a finely banded biotite-rich gneiss derived principally from porphyritic monzogranite (adamellite); and the Dugel gneiss, a leucocratic syenogranitic gneiss which intrudes and is interfolded with the Meeberrie gneiss. Both have a more complex history of deformation than the metasediments and have therefore been interpreted to be older. Immediately adjacent to Mt Narryer they have given zircon crystallization ages of *ca* 3680 Ma (Meeberrie gneiss) and 3380 Ma (Dugel gneiss), as well as a 3300 Ma age for younger zircon overgrowths (Kinny *et al* 1988a). Additionally, the Dugel gneiss is host to remnants of a 3730 Ma layered anorthosite–gabbro–ultramafic intrusion

*Present address: ZWO Laboratorium voor Isotopen-Geologie, De Boelelaan 1085, 1081 HV Amsterdam, The Netherlands.

†Present address: NZAAA, PO Box 741, Wellington, New Zealand.

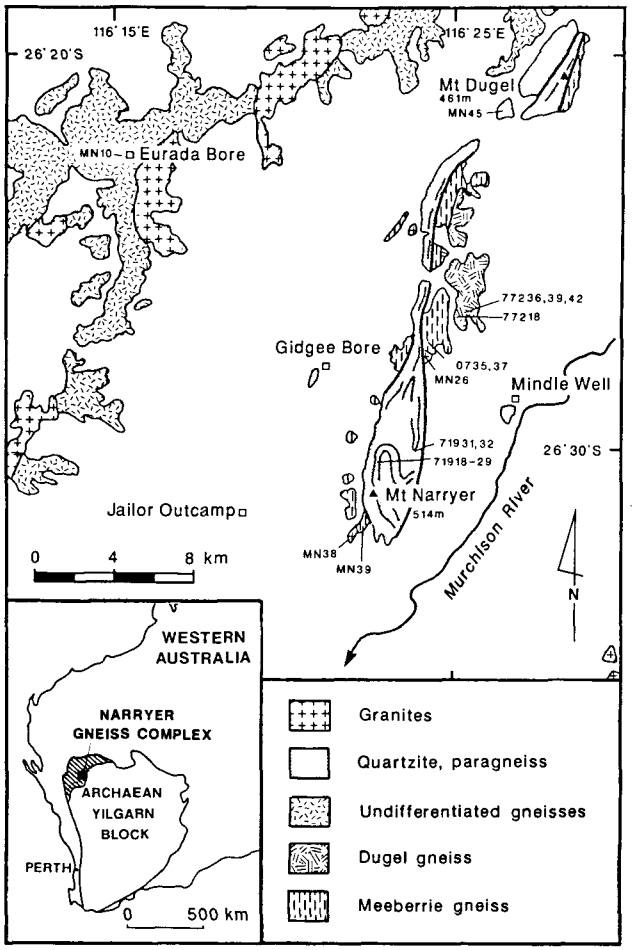

Fig. 1 Simplified geological map of the Narryer Gneiss Complex in the vicinity of Mt Narryer, indicating localities of samples discussed in the text. Undifferentiated gneisses includes one dated locality of orthogneiss at Eurada Bore, sample MN10, which gave a zircon age of 3483 ± 4 Ma (Kinny 1987).

known as the Manfred Complex, described in detail by Myers (1988b).

Three major episodes of deformation affecting the orthogneisses at Mt Narryer were recognized by Myers and Williams (1985): D_1, which produced gneissose banding in the Meeberrie gneiss; D_2, which deformed both Meeberrie and Dugel gneisses together and produced a flaser deformation fabric parallel to banding; and D_3, an episode of large-scale refolding. Present in the Narryer metasediments are simpler deformation structures, dominated by a major south-plunging syncline refolded on the eastern limb into a tight antiform. In some places sedimentary structures are well preserved. The margins of the quartzite are zones of intense deformation, leading to uncertainty in the correlation of structures (Myers & Williams 1985). Prograde metamorphic mineral assemblages in Archaean rocks of the Narryer region range from amphibolite to granulite facies associations, all of which have recrystallized to some extent at greenschist facies.

ANALYTICAL METHODS

The high resolution ion microprobe technique for U–Th–Pb dating of zircons was described by Compston *et al* (1984), with subsequent modifications outlined by Kinny *et al* (1988a). Following a review of the conventionally measured isotopic composition of laboratory standard SL3, Pb/U ratios of unknown zircons are now determined by normalization to a radiogenic $^{206}Pb/^{238}U$ for SL3 of 0.0928, a 3.8% increase on the previously used value of 0.0894. All data obtained using the old value should be adjusted by a factor of 1.038 to the radiogenic Pb/U and Pb/Th ratios, with Th/U and Pb isotopic compositions remaining unchanged. The data presented here are corrected for common Pb, using the observed ^{204}Pb abundance and either a common Pb composition assumed to be that of Broken Hill ore Pb (when surface contaminants are dominant) or a modelled intrinsic common Pb appropriate to the indicated age (Cumming & Richards 1975).

The technique for conventional K–Ar dating was described by McDougall and Schmincke (1977), and for $^{40}Ar/^{39}Ar$ analysis by McDougall (1974) and McDougall and Roksandic (1974). Samples for $^{40}Ar/^{39}Ar$ analysis were irradiated for two full 21 day cycles of the HIFAR reactor of the Australian Atomic Energy Commission. Correction factors for interference of Ar isotopes produced from activated isotopes of K and Ca were reported by Tetley *et al* (1980). The measured abundances of ^{37}Ar and ^{39}Ar formed during irradiation were corrected using the modified equation of Wijbrans (1985) for radioactive decay during the period before analysis.

Samples prefixed 'MN' were collected in 1983 by PDK during fieldwork undertaken in collaboration with the Geological Survey of Western Australia. The remaining samples, identified by a five-digit number, either were supplied by GSWA geologists J. S. Myers and I. R. Williams or were recollected from their original localities. The values for decay constants and isotopic abundances are those recommended by the IUGS (Steiger & Jäger 1977).

ZIRCON DATA

At the 25 μm scale of analysis (cf. typical grain-size of igneous zircon 250×100 μm), each zircon sample yields a diversity of isotopic compositions.

Geological interpretations of the isotopic data are based upon observations of crystal morphology. Selection criteria for age calculations are the Pb/U age concordance and the uranium content of individual analyses. High-U parts of crystals, which accumulate damage faster than other areas and which therefore may respond to earlier geological disturbances, are generally excluded.

Mt Narryer quartzite

So far the isotopic compositions of 275 individual zircon grains from the Mt Narryer quartzite sequence have been determined using the ion microprobe (Froude *et al* unpubl. data, 1983). These grains were extracted from three separate localities within the sequence (GSWA localities 71921, 71924 and 71932; Fig. 1). The host rock in each case was an orthoquartzite. Two samples (71921, 24) are petrographically similar, featuring quartz associated with sillimanite, cordierite, biotite and garnet. The third sample (71932), in which 4100–4200 Ma zircons were first found, has a different assemblage of quartz with minor calcic plagioclase (bytownite) and biotite, secondary zoisite and sericite. A further 39 whole zircon grains and grain fragments from sample 71932 have been analysed using thermal ionization mass spectrometry (Schärer & Allègre 1985). A graphical comparison of the results of both techniques is given in Fig. 2, which illustrates: (1) the excellent agreement between both techniques in definition of the principal age populations (3300–3700 Ma); (2) the rarity of the 4100–4200 Ma zircons (seven grains); and (3) the overall non-zero age discordance trajectory. The field defined by the ion probe analyses includes all the analyses by Schärer and Allègre (1985), and extrapolates to between 1000 and 1500 Ma on the lower part of the concordia curve.

Froude *et al* (1983) ascribed a detrital origin to those grains which yielded ages ⩾3500 Ma and a metamorphic origin to those with ages of 3300 and 3100 Ma, implying that the sedimentary sequence was deposited during the interval 3500 to 3300 Ma. This division was not based on any morphological or chemical distinctions between the apparent age populations; it was based purely on an assumption that the 3348 ± 43 Ma Rb–Sr isochron age which had been obtained from the adjacent orthogneisses (de Laeter *et al* 1981) registered the time of for-

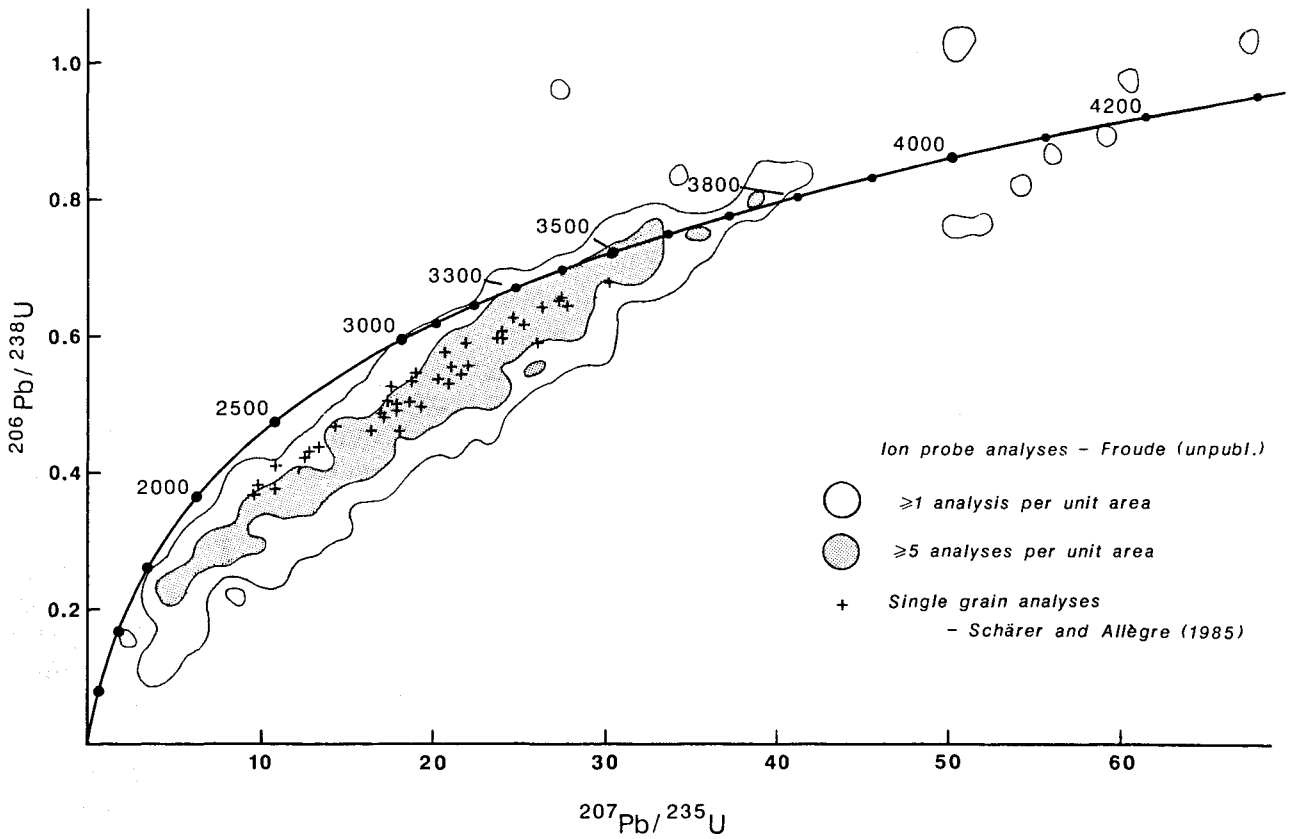

Fig. 2 Concordia plot of all U–Pb analyses of detrital zircons from the Mt Narryer quartzite. For clarity, the 275 ion probe analyses have been contoured over a unit area the size of the circle used in the key on the diagram, and the orthodox single grain and grain-fragment analyses superimposed as crosses. Ages are in Ma.

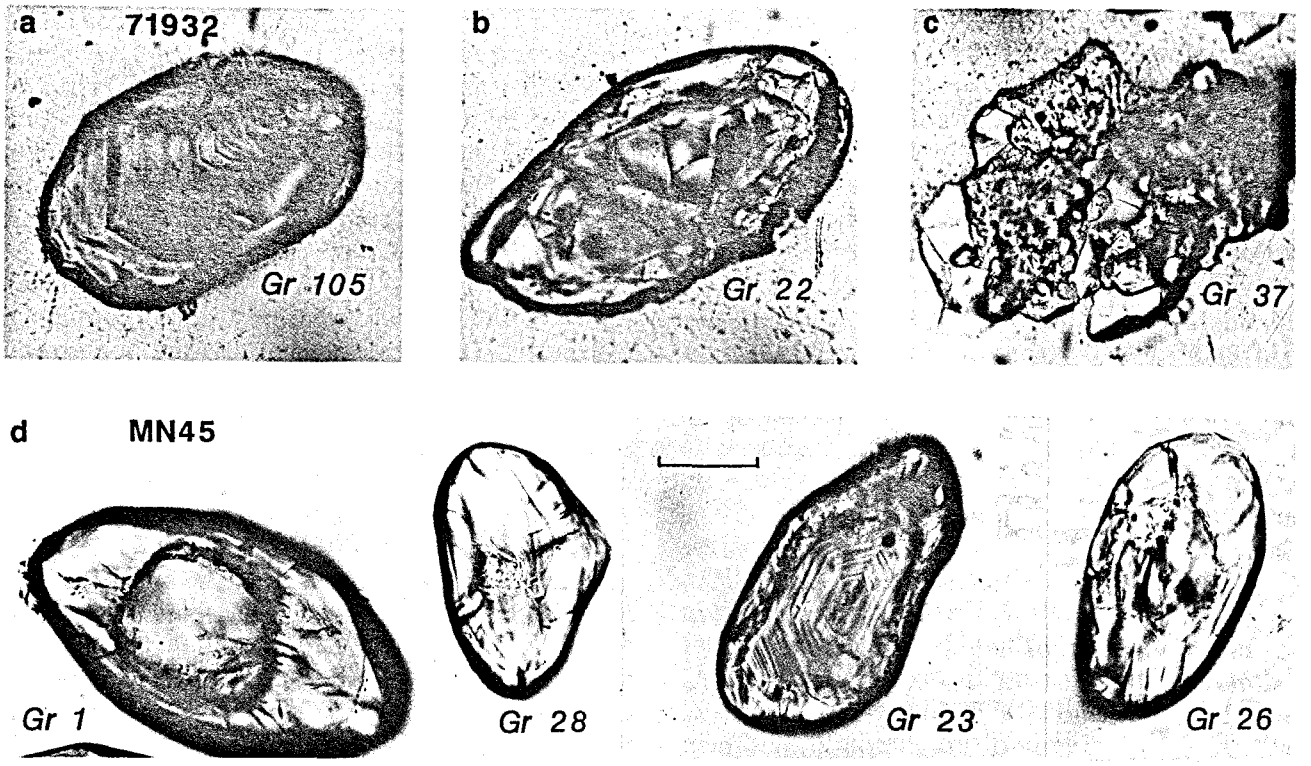

Fig. 3 (a)–(c) Transmitted light photomicrographs of selected zircons from the Mt Narryer quartzite, sample 71932. (d) Four zircons from pelitic paragneiss west of Mt Dugel, sample MN45. Scale bar = 50 μm.

mation of the high-grade mineral assemblages both in the orthogneisses themselves and in the metasediments. Morphologically, the younger grains are indistinguishable from the rest, most younger grains displaying the euhedral internal zonation usually present in melt derived grains. Three grains with exceptional morphology (grains 37, 201, 202) occur as clusters of small round crystals intergrown with quartz and mica (Fig. 3c), but all three are metamict and give highly discordant U–Pb ages so that their original ages and origin are indeterminate. Nevertheless, the surface features which might be expected on detrital grains in water-lain deposits (such as pitting caused by mechanical abrasion) are generally absent; instead smooth metamorphic rounding and corrosion has affected all grains to the extent that any pre-existing surface textures would have been erased. The only clear instances of younger metamorphic overgrowths on older grains are the rims *ca* 3.90 Ga in age which have been identified on four of the 4.20 Ga zircons.

If all of the zircon grains in the quartzite were indeed detrital, and if the youngest ages could be substantiated, a major revision of the established geological history of the region would be necessary — especially the supposed relation between the quartzite sequence and the adjacent orthogneiss terrane, and the timing of episodes of metamorphism. Accordingly, up to three new areas on each of the ten apparently youngest zircons from sample 71932 have been analysed. Results are given in Table 1, along with the original data for each grain (Froude unpubl.) and results for grains 201 and 202 (not previously analysed). Figure 4 gives the positions of all these analyses as 1σ error boxes on a standard Pb/U concordia diagram. On Fig. 4, data points with U contents above an arbitrary value of 800 parts/10^6 have been distinguished from those below, to emphasise the relation between U content and Pb/U age discordance that exists amongst these grains as indeed within single crystals.

Grains 104 and 105 (Fig. 3a) both are clear, sub-rounded grains with euhedral zonation and abundant mineral inclusions. Without exception, the analytical spots on these grains yielded approximately concordant Pb/U ages, with U contents in the range 305–675 parts/10^6. The mean radiogenic $^{207}Pb/^{206}Pb$ of the four analyses of grain 104 corresponds to an apparent age of 3303 ± 10 Ma, whereas grain 105 gives 3281 ± 14 Ma (2σ).

Grains 22 (Fig. 3b), 88 and 125 display more varied internal structures, each including both clear, finely zoned areas and darker, turbid areas. Analyses of these grains ranged from near-

Table 1 Results of ion probe U–Th–Pb analyses of young zircons in the Mt Narryer quartzite, Western Australia (sample 71932).

Grain–Spot	$^{207}Pb/^{206}Pb$	$^{206}Pb/^{238}U$	$^{207}Pb/^{235}U$	$^{208}Pb/^{206}Pb$	Th/U	$U/10^6$	Raw 6/4	%comm. ^{206}Pb	7/6 Age (Ma)
22–1	0.2321 ± 9	0.471 ± 14	15.1 ± 0.4		0.242	850			3067
2	0.2687 ± 13	0.604 ± 6	22.4 ± 0.3	0.0418 ± 21	0.147	783	900	1.78	3298
4	0.2685 ± 14	0.611 ± 6	22.6 ± 0.3	0.1980 ± 25	0.664	565	910	1.77	3297
23–1	0.2384 ± 8	0.562 ± 16	18.5 ± 0.5		0.092	1312			3109
2	0.2392 ± 10	0.618 ± 6	20.4 ± 0.2	0.0621 ± 14	0.211	865	1800	0.90	3114
3	0.2552 ± 13	0.558 ± 6	19.7 ± 0.2	0.1227 ± 19	0.527	631	1900	0.85	3217
32–1	0.2341 ± 17	0.553 ± 16	17.9 ± 0.5		0.051	1002			3080
2	0.1982 ± 8	0.408 ± 4	11.1 ± 0.1	0.0195 ± 12	0.059	1216	1800	0.91	2811
3	0.2311 ± 11	0.492 ± 5	15.7 ± 0.2	0.0208 ± 18	0.059	1010	910	1.77	3060
33–1	0.2414 ± 29	0.508 ± 15	16.9 ± 0.5		0.133	1408			3129
2	0.1923 ± 7	0.393 ± 4	10.4 ± 0.1	0.0223 ± 10	0.066	1831	2100	0.77	2762
3	0.1951 ± 5	0.581 ± 6	15.6 ± 0.2	0.2674 ± 9	1.077	2597	1100	1.40	2786
37–1	0.1765 ± 24	0.417 ± 12	10.2 ± 0.3		0.063	1723			2620
2	0.1969 ± 10	0.446 ± 4	12.1 ± 0.1	0.0217 ± 17	0.068	1292	1200	1.38	2800
3	0.1770 ± 9	0.399 ± 4	9.7 ± 0.1	0.0139 ± 16	0.052	1309	1900	0.85	2625
4	0.1825 ± 11	0.411 ± 4	10.3 ± 0.1	0.0245 ± 21	0.066	1301	700	2.30	2676
38–1	0.1917 ± 28	0.354 ± 10	9.4 ± 0.3		0.119	1866			2757
2	0.2509 ± 5	0.572 ± 6	19.8 ± 0.2	0.1464 ± 18	0.110	1756	350	4.64	2953
3	0.2585 ± 7	0.559 ± 6	19.9 ± 0.2	0.0238 ± 7	0.087	1251	4100	0.39	3238
88–1	0.2591 ± 15	0.629 ± 18	22.5 ± 0.7		0.239	817			3241
2	0.2270 ± 8	0.461 ± 5	14.4 ± 0.2	0.0434 ± 11	0.105	1281	1800	0.88	3031
3	0.0927 ± 40	0.297 ± 3	3.8 ± 0.2		0.198	1824	230	6.96	1483
104–1	0.2645 ± 25	0.619 ± 17	22.6 ± 0.7		0.532	359	2400	0.67	3274
2	0.2690 ± 16	0.700 ± 7	26.0 ± 0.3	0.1077 ± 23	0.415	579	1800	0.91	3300
3	0.2599 ± 30	0.683 ± 7	24.5 ± 0.4	0.1310 ± 54	0.522	305	610	2.64	3246
4	0.2730 ± 13	0.689 ± 7	25.9 ± 0.3	0.1399 ± 19	0.507	455	2000	0.82	3323
105–1	0.2750 ± 32	0.630 ± 18	23.9 ± 0.7		0.587	625	3600		3335
2	0.2613 ± 33	0.654 ± 6	23.6 ± 0.4	0.1202 ± 58	0.485	237	560	2.86	3254
3	0.2666 ± 20	0.671 ± 6	24.7 ± 0.3	0.1676 ± 30	0.626	448	1500	1.06	3286
4	0.2642 ± 15	0.629 ± 6	22.9 ± 0.3	0.1504 ± 19	0.579	674	2800	0.57	3272
125–1	0.2652 ± 7	0.658 ± 11	24.1 ± 0.4		1.050	635	8900	0.18	3278
2	0.2320 ± 9	0.460 ± 4	14.7 ± 0.2	0.2734 ± 14	0.902	1115	2700	0.59	3066
3	0.2419 ± 10	0.512 ± 5	17.1 ± 0.2	0.2262 ± 15	0.742	839	2800	0.58	3133
201–1	0.1691 ± 13	0.352 ± 4	8.2 ± 0.1	0.0701 ± 25	0.246	1287	560	2.84	2549
202–1	0.1991 ± 6	1.078 ± 11	29.6 ± 0.3	0.3707 ± 11	2.164	1565	910	1.76	2820

For all grains except 201 and 202, spot 1 is an analysis by Froude *et al* (1983) with an estimated 3% precision in $^{206}Pb/^{238}U$. For most of these analyses, records are not available of the $^{208}Pb/^{206}Pb$ and %common ^{206}Pb. All other data are 1986 analyses at *ca* 1% precision in $^{206}Pb/^{238}U$. 1σ errors. Data were corrected for common Pb using the measured $^{204}Pb/^{206}Pb$ and assuming Broken Hill ore Pb composition ($^{204}Pb/^{206}Pb = 0.0625$, $^{207}Pb/^{206}Pb = 0.9618$, $^{208}Pb/^{206}Pb = 2.2285$).

concordant to highly discordant compositions. A line of best fit drawn through the three analyses of grain 22 intersects the concordia curve at ages of 3383 and 1451 Ma. A similar treatment of the data for grain 125 yields intercepts of 3281 and 1146 Ma. Because they are based on small data sets these regression lines are somewhat arbitrary, but they are parallel to the average discordance trajectory of the complete data set (cf Fig. 2), and their upper concordia intercepts are controlled by near-concordant, relatively low-U analyses so probably are close to the original ages of the grains. However, a reasonable line cannot be drawn through all three data points from grain 88. Joining spots 1 and 2 alone yields a chord with intercepts of 3266 and 1221 Ma, whereas spot 3, with a very high U content of over 1800 parts/10^6 U, plots slightly above concordia at an apparent $^{207}Pb/^{206}Pb$ age of *ca* 1500 Ma.

The remaining grains under consideration yielded only highly discordant isotopic compositions. They comprise a variety of pristine and

altered grains, averaging in excess of 1000 parts/10^6 U where analysed. By virtue of their discordant compositions they cannot be claimed with confidence to be older or younger than the grains described above. Two exceptional analyses, 33-3 and 202-1 (not shown on Fig. 4), plot well above the concordia curve. Both are characterized by Th contents in excess of 2500 parts/10^6, perhaps due to unidentified inclusions. If so, the high Pb/U ratios would be spurious because the empirical Pb/U calibration process for zircon does not extend to analyses of spots which include foreign inclusions with different matrix compositions. Alternatively, there may locally be genuine deficiencies of the radioactive parent elements in these most disturbed domains. Other spots on grain 33 have low Th/U and are discordant in the usual sense.

In summary, the youngest grains in sample 71932 for which ages can be determined with confidence are evidently 3280 to 3300 Ma old. These young grains are no different in appearance from many other zircons in the sample which give older ages and which are considered to be detrital in origin. Previously reported apparent ages of 3100 Ma from this sample (Froude *et al* 1983) are shown here to be artifacts of ancient disturbances to the Pb isotopic compositions of high-U parts of older grains. Judging from the typical discordance trajectories, loss of radiogenic Pb from these domains took place at least as early as 1500 Ma.

Mt Dugel paragneiss

The Mt Narryer quartzite can be traced discontinuously across shear zones to include prominent exposures at Mt Dugel to the north and possibly also Mt Murchison to the south. Whereas at most localities the quartzite sequence is bounded by felsic gneisses of demonstrably igneous origin, on the western side of Mt Dugel the sequence adjoins a series of garnet-bearing felsic gneisses which may be paragneisses, interleaved with lenses of micaceous quartzite, banded iron formation and rare mafic gneisses. About 3.5 km west-southwest of the summit of Mt Dugel a 30 m wide meta-pelitic horizon is exposed over a distance of 400 m. The exposure includes both a fine grained hypersthene–anorthite–quartz rock and a distinctive porphyroblastic horizon (sample MN45) composed of hypersthene and almandine garnet phenocrysts,

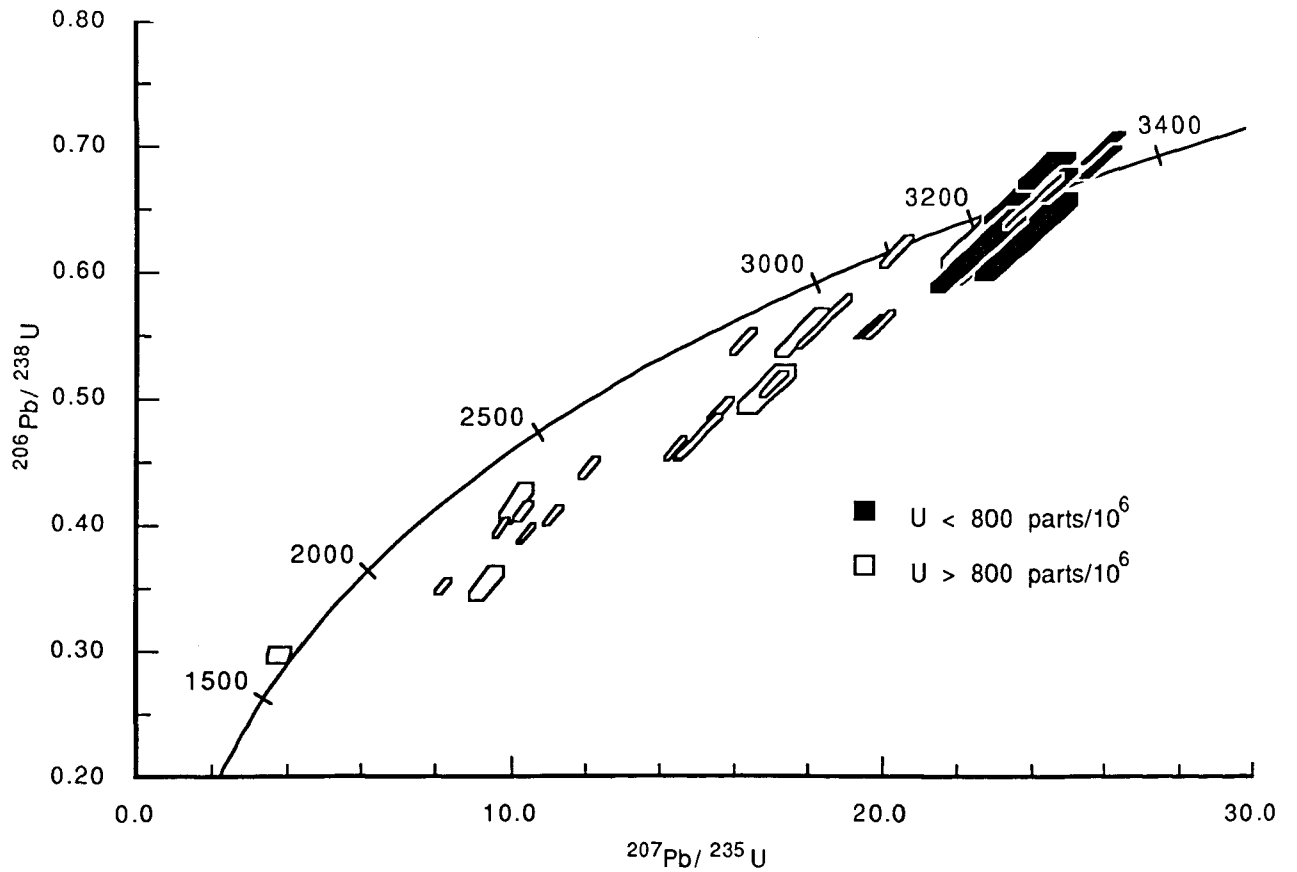

Fig. 4 Concordia plot of ion probe analyses of the youngest zircons in the Mt Narryer quartzite, sample 71932. Data from Table 1, represented as 2σ error boxes. Marked ages in Ma.

up to 10 mm in diameter, set in a matrix of cordierite–biotite–quartz with accessory magnetite/ilmenite and zircon. As a representative of the high-grade metasedimentary suite, zircon analyses from MN45 provide important additional information about the geological evolution of the region because, unlike the zircons from the Mt Narryer quartzites, virtually every zircon extracted from this rock exhibits an isotopically distinct core–rim relationship. The majority are small sub-rounded grains less than 60 μm in diameter, a size expected within what was once a fine grained sediment. A number of representative grains are illustrated in section in Fig. 3d. Each exhibits a distinct rounded or broken structural core surrounded by an optically homogeneous rim. Grain 23 (Fig. 3d) is a particularly fine example of a euhedrally zoned detrital core presumably of igneous origin, separated by a sharp, jagged margin from the structureless enclosing mantle.

Where possible, the chosen grains were analysed in both core and rim areas. Analyses of sixteen cores revealed a wide range in U and Th contents and in isotopic compositions (Table 2). The majority have near-concordant Pb/U ages, plotting just below the concordia curve (solid symbols, Fig. 5). Three grains yielded rather more discordant compositions (grains 4, 5 and 26), these being the lowest in $^{207}Pb/^{206}Pb$. Among the near-concordant analyses $^{207}Pb/^{206}Pb$ ages range from 3500 ± 9 Ma (grain 3), through 3252 ± 29 Ma (grain 8), 3190 ± 13 Ma (grain 15) and 3182 ± 8 Ma (grain 9) to a cluster of analyses with ages of *ca* 3100 Ma. In contrast, the nine analysed rims were uniformly low in Th/U (<0.07) and relatively uniform in isotopic composition. Indicated $^{207}Pb/^{206}Pb$ ages are consistently younger than for the enclosed cores, the lowest values again coming from discordant analyses (grains 2, 3 and 8), implying a component of ancient Pb loss in the isotopic evolution of core and rim areas alike. The most concordant rim analyses combine to a mean $^{207}Pb/^{206}Pb$ age of 2683 ± 8 Ma (2σ). The rim on grain 12 was exceptional in having over 2000 parts/10^6 U at the

Table 2 Results of ion probe U–Th–Pb analyses of zircons from pelitic paragneiss 3.5 km west-southwest of Mt Dugel, Western Australia (sample MN45).

Grain–Spot	$^{207}Pb/^{206}Pb$	$^{206}Pb/^{238}U$	$^{207}Pb/^{235}U$	$^{208}Pb/^{206}Pb$	Th/U	U/10^6	Raw 6/4	%comm. ^{206}Pb	7/6 Age (Ma)
Rounded detrital cores									
3–1	0.3059 ± 8	0.705 ± 7	29.7 ± 0.3	0.2917 ± 8	1.108	370	11 800	0.13	3500
8–1	0.2609 ± 24	0.588 ± 8	21.2 ± 0.3	0.1724 ± 38	0.580	114	9500	0.25	3252
15–1	0.2509 ± 10	0.603 ± 8	20.8 ± 0.3	0.1674 ± 10	0.615	391	6400	0.19	3190
9–1	0.2496 ± 6	0.588 ± 7	20.2 ± 0.3	0.0096 ± 4	0.036	905	16 200	0.08	3182
10–1	0.2382 ± 6	0.586 ± 7	19.2 ± 0.2	0.1289 ± 6	0.470	981	11 100	0.12	3108
23–1	0.2382 ± 7	0.571 ± 7	18.8 ± 0.2	0.1616 ± 8	0.584	658	11 300	0.12	3108
13–1	0.2381 ± 9	0.580 ± 7	19.0 ± 0.3	0.3316 ± 13	1.197	500	27 600	0.07	3107
25–1	0.2374 ± 11	0.555 ± 7	18.2 ± 0.2	0.1785 ± 13	0.642	326	4500	0.30	3102
24–1	0.2348 ± 13	0.580 ± 8	18.8 ± 0.3	0.0890 ± 18	0.313	284	5100	0.27	3085
1–1	0.2339 ± 7	0.548 ± 6	17.7 ± 0.2	0.2336 ± 9	0.803	356	8600	0.16	3079
12–1	0.2336 ± 8	0.560 ± 7	18.0 ± 0.2	0.2054 ± 10	0.737	588	7100	0.18	3077
2–1	0.2324 ± 7	0.549 ± 6	17.6 ± 0.2	0.1518 ± 8	0.531	417	6700	0.23	3068
6–1	0.2288 ± 11	0.519 ± 7	16.4 ± 0.2	0.1607 ± 14	0.551	296	8800	0.24	3044
26–1	0.2123 ± 13	0.503 ± 7	14.7 ± 0.2	0.1421 ± 20	0.466	214	2300	0.59	2923
4–1	0.1977 ± 7	0.428 ± 4	11.7 ± 0.1	0.0513 ± 7	0.154	474	7300	0.19	2808
5–1	0.1830 ± 9	0.409 ± 5	10.3 ± 0.1	0.0530 ± 11	0.172	384	6120	0.26	2680
Metamorphic rims									
27–2	0.1844 ± 8	0.494 ± 6	12.6 ± 0.2	0.0041 ± 8	0.016	586	15 000	0.13	2692
5–2	0.1830 ± 12	0.475 ± 6	12.0 ± 0.2	0.0039 ± 15	0.023	288	4000	0.42	2681
1–2	0.1829 ± 6	0.495 ± 5	12.5 ± 0.1	0.0128 ± 6	0.056	464	7300	0.19	2680
24–2	0.1826 ± 10	0.505 ± 7	12.7 ± 0.2	0.0151 ± 8	0.067	345	4900	0.35	2677
12–2	0.1804 ± 4	0.530 ± 7	13.2 ± 0.2	0.0023 ± 2	0.007	2063	>10^5	0.02	2657
4–2	0.1793 ± 7	0.478 ± 5	11.8 ± 0.1	0.0028 ± 5	0.012	588	14 700	0.13	2647
3–2*	0.1686 ± 7	0.406 ± 5	9.4 ± 0.1	0.0577 ± 6	0.159	641	8300	0.17	2544
2–2	0.1642 ± 6	0.427 ± 4	9.7 ± 0.1	0.0043 ± 6	0.025	501	6400	0.22	2499
8–2	0.1502 ± 5	0.365 ± 5	7.6 ± 0.1	0.0017 ± 4	0.007	1335	13 300	0.11	2348

*Composite (>80% rim).

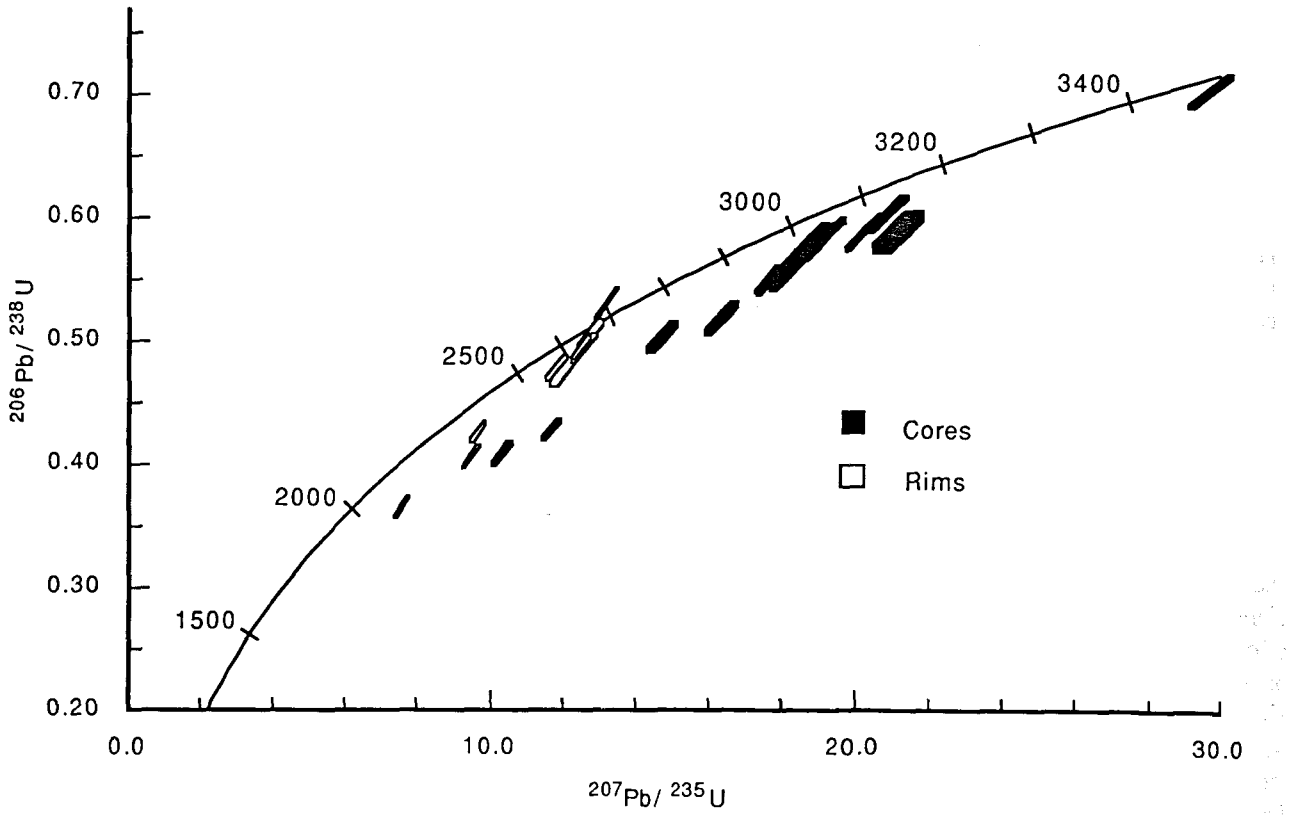

Fig. 5 Concordia plot of ion probe analyses of zircons from pelitic paragneiss west of Mt Dugel, sample MN45. Data from Table 2, represented as 2σ error boxes. Marked ages in Ma.

analysed location and reversely discordant Pb/U isotopic ratios. In this instance, given the lack of evidence for inclusions, this result must be considered as a real consequence of loss of U relative to Pb. The $^{207}Pb/^{206}Pb$ ratio is only marginally lower than that of the low-U rims, implying that the movement probably occurred in the relatively recent past.

Based on the available data, the zircons from MN45 are interpreted as a composite detrital population derived predominantly from igneous lithologies formed between 3100 and 3500 Ma ago, which were deposited as sediment after 3100 Ma, and which subsequently were overgrown by new zircon *in situ*, *ca* 2680 Ma. The consistently low Th/U of the younger rims has been identified elsewhere as a feature of metamorphic overgrowths of zircon in high-grade rocks (e.g. Williams & Claesson 1987).

Porphyritic granite intrusion

A porphyritic granite is exposed over an area of 8 ha, immediately to the east of the Narryer quartzite range and 1 km south of the type-locality for the Meeberrie gneiss (sample MN26, Fig. 1). Although lacking the penetrative (D_1) banding of the Meeberrie gneiss which it intrudes, the granite possesses a (D_2) flaser deformation fabric. Additionally, the granite is intensively deformed on its western margin by the mylonite zone marking the boundary of the metasedimentary sequence. In thin section, ragged green biotite laths are oriented along the boundaries of perthitic K-feldspar augen, and quartz grains have undulose extinction and partial recrystallization to finer grained aggregates.

This granite occupies an extremely important position in the geological record of the Mt Narryer region, representing a widespread episode of granite injection. According to Myers and Williams (1985), growth of metamorphic pyroxenes in D_2 tectonic fabrics throughout the Mt Narryer region indicates that granulite facies metamorphism was synchronous with the D_2 episode. Emplacement of this porphyritic granite clearly post-dates D_1 deformation but predates D_2, the associated metamorphism and the movement on the shear zone which brought the sediments and orthogneisses to their present juxtaposition. Further exposures of porphyritic granite of as yet unknown affiliation are present on the western side of the Narryer range, 6 km north of this locality.

Zircon is abundant in sample MN26 within the feldspars and at feldspar–quartz boundaries, in

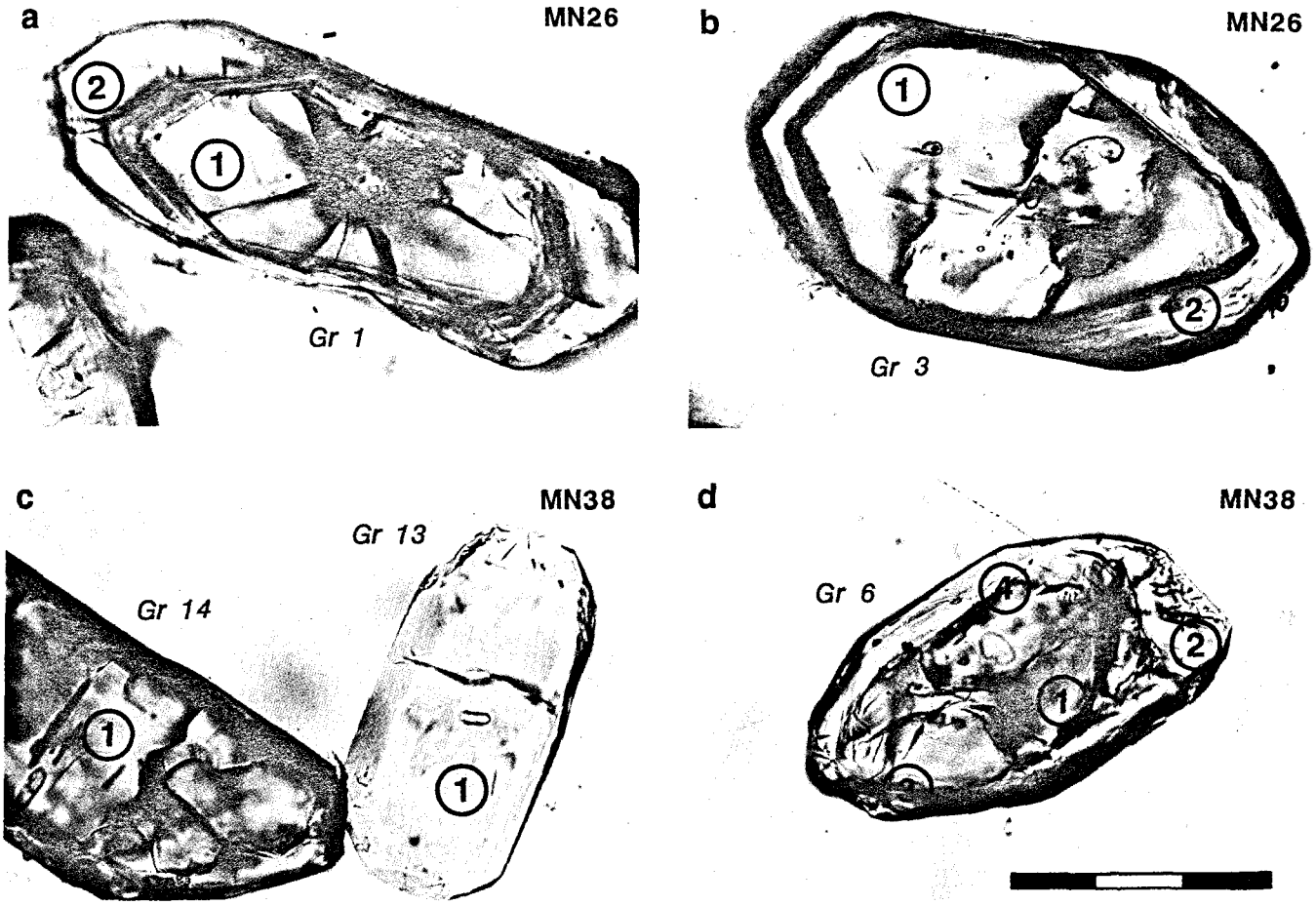

Fig. 6 (a, b) Zircons from porphyritic granite MN26, showing euhedral cores surrounded by finely zoned rims. The inner core of grain 1 is a highly metamict phase and is responsible for the radial cracking pattern. Positions of ion probe analytical spots are shown. (c, d) Zircons from fine-grained granite southwest of Mount Narryer (MN38). Grains 6 and 14 each contain an irregular structural core, whereas grain 13 is a wholly igneous grain. Scale bar divisions: 50 μm for all photographs.

contrast to accessory sphene and opaque phases which are associated with biotite. The zircons are a coherent population of elongate euhedral grains, each consisting of a poorly zoned inclusion-rich core overgrown by a strongly zoned rim (Fig. 6a, b). The core–rim boundary is euhedral, with no apparent structural discontinuity. Some grains have in their core a small altered centre (e.g. grain 1, Fig. 6a) while others have nucleated on acicular apatite.

The results of ion probe analyses of core and rim areas in eleven grains from MN26 are given in Table 3. Analyses of the cores fall into two groups, the majority registering distinctly low U levels (<200 parts/10^6 U), in contrast to two dark cores with turbid appearance (grains 11, 12) both of which registered over 1200 parts/10^6 U. As indicated in Fig. 7, the low-U cores are 0–10% discordant at an indicated age of *ca* 3300 Ma, implying minor recent Pb loss. The combined $^{207}Pb/^{206}Pb$ age of all nine low-U cores is 3302 ± 6 Ma (2σ). The two high-U cores are highly discordant, spot 12–2 having a much lower $^{207}Pb/^{206}Pb$ than the above, and spot 11–2 having a slightly higher $^{207}Pb/^{206}Pb$.

The results of analyses of the finely zoned rims (Table 3) indicate that on average they contain higher levels of U than the low-U cores but have similar Th contents and hence a lower Th/U ratio. The rim analyses also are much higher in intrinsic common Pb than are most cores, but because of the higher U content of the rims, the common Pb as a fraction of the total ^{206}Pb is similar in both. Spot 5–2 has a radiogenic $^{207}Pb/^{206}Pb$ ratio indistinguishable from that of the low-U cores, supporting the interpretation based on morphology that there may be no significant difference between the original age of cores and rims. The other rims, to varying degrees, have a lower $^{207}Pb/^{206}Pb$ ratio, having apparently suffered early Pb loss, although a number of these remain near-concordant.

The zircons from MN26 appear to be entirely igneous grains. The lack of growth-zoning in the majority of cores is attributed to their relatively low

Table 3 Ion probe analyses of zircons from porphyritic granite intruding Meeberrie gneiss east of Mt Narryer, Western Australia (sample MN26).

Grain–Spot	$^{207}Pb/^{206}Pb$	$^{206}Pb/^{238}U$	$^{207}Pb/^{235}U$	$^{208}Pb/^{206}Pb$	Th/U	$U/10^6$	Raw 6/4	%comm. ^{206}Pb	7/6 Age (Ma)
Cores									
11–2	0.2757 ± 4	0.464 ± 6	17.6 ± 0.2	0.0193 ± 3	0.072	1349	10 300	0.13	3338
8–1	0.2713 ± 17	0.605 ± 9	22.6 ± 0.4	0.3492 ± 32	1.141	137	550	2.32	3314
2–1	0.2701 ± 13	0.608 ± 8	22.6 ± 0.3	0.3392 ± 21	1.205	192	910	1.35	3306
6–1	0.2699 ± 19	0.564 ± 8	21.0 ± 0.3	0.3641 ± 35	1.190	121	590	2.25	3305
4–1	0.2695 ± 15	0.622 ± 9	23.1 ± 0.4	0.1769 ± 19	0.660	124	3700	0.44	3303
10–2	0.2692 ± 12	0.630 ± 9	23.4 ± 0.4	0.2519 ± 16	0.951	148	4500	0.33	3301
9–2	0.2691 ± 17	0.620 ± 9	23.0 ± 0.4	0.1640 ± 21	0.624	100	2800	0.61	3301
1–1	0.2678 ± 27	0.567 ± 9	20.9 ± 0.4	0.2429 ± 49	0.826	62	580	2.25	3293
3–1	0.2674 ± 18	0.639 ± 10	23.6 ± 0.4	0.3203 ± 27	1.211	78	3000	0.51	3291
5–1	0.2665 ± 23	0.620 ± 10	22.8 ± 0.4	0.2127 ± 35	0.809	56	1700	0.82	3285
12–2	0.2223 ± 6	0.368 ± 5	11.3 ± 0.2	0.0224 ± 10	0.025	1204	970	1.31	2997
Rims									
5–2	0.2683 ± 10	0.592 ± 8	21.9 ± 0.3	0.0474 ± 16	0.076	430	670	1.82	3296
12–1	0.2661 ± 7	0.633 ± 8	23.2 ± 0.3	0.0381 ± 8	0.119	555	1700	0.73	3283
10–1*	0.2661 ± 9	0.604 ± 8	22.2 ± 0.3	0.0621 ± 15	0.139	558	490	2.56	3283
3–2	0.2619 ± 7	0.613 ± 8	22.1 ± 0.3	0.0329 ± 8	0.098	491	2400	0.52	3258
11–1	0.2609 ± 10	0.559 ± 8	20.1 ± 0.3	0.0467 ± 14	0.128	331	1000	1.26	3252
4–2	0.2554 ± 7	0.580 ± 8	20.4 ± 0.3	0.0267 ± 9	0.056	740	1300	0.98	3218
2–2	0.2548 ± 6	0.576 ± 8	20.2 ± 0.3	0.0112 ± 5	0.032	541	5900	0.21	3215
1–2	0.2493 ± 7	0.511 ± 7	17.6 ± 0.2	0.0541 ± 10	0.109	821	1000	1.29	3180
11–3*	0.2135 ± 9	0.324 ± 4	9.6 ± 0.1	0.0600 ± 17	0.095	1026	420	2.92	2932
9–1	0.1190 ± 8	0.197 ± 3	3.2 ± 0.1	0.1799 ± 17	0.273	1601	440	2.86	1941

Modelled intrinsic 3300 Ma-old common Pb used for data correction (Cumming & Richards 1975).
*Composite (>80% rim).

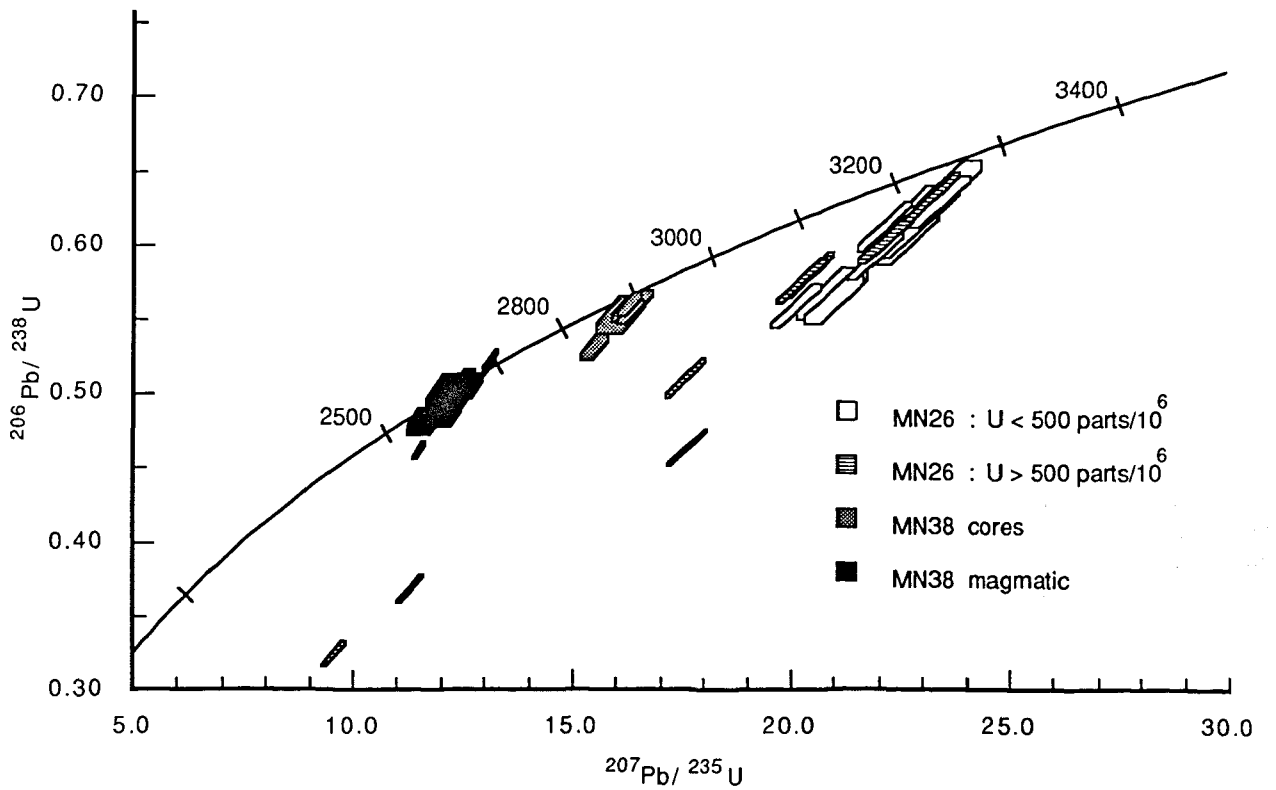

Fig. 7 Combined concordia plot of ion probe zircon analyses from both intrusive granites (porphyritic MN26, fine grained MN38). Data from Tables 3 and 4, represented as 2σ error boxes. Marked ages in Ma.

and uniform U contents, in contrast to the zoned rims which evidently represent more highly trace-element substituted domains added during the later stages of the same episode of magmatic crystallization. Given the 25 μm spatial resolution of the ion beam, each rim analysis must be considered as giving an average composition of many such domains. The range of present-day Pb/U isotopic compositions identified at this scale of analysis highlights the potential for contrasting responses of low-U and high-U parts of zircons from a simple cogenetic population to geological processes over time. Only the low-U cores preserve a precise crystallization age, 3302 ± 6 Ma.

Fine grained granite intrusion

Fine-grained foliated granite sheets intrude outcrops of Meeberrie gneiss west and southwest of Mt Narryer. They are biotite adamellites with equigranular textures and only minor recrystallization at grain boundaries. De Laeter *et al* (1985) sampled these granites and obtained an Rb–Sr isochron age of 2579 ± 122 Ma (MSWD 0.31) and an Sm–Nd T_{CHUR} model age on one sample of 3120 ± 30 Ma. They also obtained a comparable Sm–Nd model age of 3070 ± 40 Ma from a granite of similar appearance which intrudes the metasedimentary belt nearby to the east. Because these granites intrude both the orthogneisses and the metasediments, knowledge of their true ages of emplacement would place a younger limit on the time at which the country rocks achieved their present tectonic configuration.

A granite 2.5 km southwest of Mt Narryer (MN38, Fig. 1) has been sampled. Accessory zircon is present throughout the mineral assemblage, but particularly is associated with pleochroic brown–green biotite grains. The zircons are brown or pale in colour and form subhedral grains, rich in mineral inclusions. A few have regular euhedral zonation but most are relatively poorly zoned. An estimated 30% of the analysed grains have distinct cores which, unlike the euhedral igneous cores described from the 3300 Ma porphyritic granite, have irregularly shaped, rounded margins indicating a hiatus in the crystallization history of these grains (Fig. 6c, d).

Isotopic data for the MN38 zircons are given in Table 4. The structural cores are remarkably uniform in isotopic composition, having the same $^{207}Pb/^{206}Pb$ ratio, low U, and a narrow range in Pb/U isotopic ratios (Fig. 7). Their mean $^{207}Pb/^{206}Pb$ age is 2919 ± 8 Ma (2σ). Analyses of the rims surrounding two of these cores (spots 6–2, 8–2) are isotopically indistinguishable from the remaining younger population. The U and Th contents of the remaining grains are highly variable, and although they all have relatively concordant isotopic compositions there is a significant spread in $^{207}Pb/^{206}Pb$ ages among them which because of the low ^{204}Pb contents of most grains cannot be assigned to an error in the common Pb correction. The highest $^{207}Pb/^{206}Pb$ ratios belong to three relatively U-rich spots (grains 3, 11 and 17) with a mean age of *ca* 2680 Ma, whereas the remaining low-U analyses give a somewhat younger mean age of 2646 ± 6 Ma (2σ). Although the cause of the scatter is unclear, the greater tendency of high-U zircon to isotopic disturbance suggests that the younger estimate of the population age, as indicated by the low-U analyses, should be preferred.

Because the older cores represent a small component of the population, and because a number of the younger grains display igneous-type zonation, the younger parts of the grains are interpreted as the magmatic population and the cores are interpreted as remnants of pre-magmatic grains inherited from the source regions of the melt. On this basis, the best estimate of the crystallization age of the granite is 2646 ± 6 Ma. This lies within the wide uncertainty of the Rb–Sr isochron age for the younger granites at Mt Narryer, 2579 ± 122 Ma (de Laeter *et al* 1985), so both systems may be registering the same event in this instance. Alternatively, there is ample scope in the Rb–Sr data for the isochron to be recording a subsequent episode of recrystallization up to 200 million years after the 2650 Ma zircon age.

ARGON DATA

A number of minerals extracted from the Mt Narryer metasediments have been analysed by the K–Ar method (results in Table 5; sample locations Fig. 1). Hornblendes from concordant quartz-rich amphibolites within the sequence (samples 71918, 71929) yielded apparent ages of 2610 ± 34 and 3664 ± 78 Ma (2σ) respectively. Biotite from 71929, which had partially altered to chlorite, gave 1789 ± 32 Ma, whereas biotite from a pelitic horizon (71931) gave 2022 ± 44 Ma. A selection of samples from the orthogneiss terrane have also been analysed. Meeberrie gneiss biotites (samples 60735, 60737) yielded apparent ages of 1887 ± 34 and 1778 ± 32 Ma. Hornblendes from leucogabbro and meta-anorthosite units (Manfred Complex) within the Dugel gneiss gave ages of 2787 ± 50 Ma (77239A) and 2667 ± 34 Ma (77236, mean of two duplicate runs). Plagioclases separated from the

Table 4 Ion probe analyses of zircons from fine grained granite 2 km southwest of Mt Narryer, Western Australia (sample MN38).

Grain–Spot	$^{207}Pb/^{206}Pb$	$^{206}Pb/^{238}U$	$^{207}Pb/^{235}U$	$^{208}Pb/^{206}Pb$	Th/U	$U/10^6$	Raw 6/4	%comm. ^{206}Pb	7/6 Age (Ma)
Magmatic zircon									
11–1	0.1834 ± 7	0.504 ± 3	12.7 ± 0.1	0.1088 ± 8	0.402	386	8600	0.26	2684
17–1	0.1833 ± 4	0.517 ± 3	13.1 ± 0.1	0.1337 ± 4	0.489	1116	27 300	0.06	2683
3–1	0.1823 ± 4	0.523 ± 3	13.1 ± 0.1	0.0214 ± 4	0.080	697	20 500	0.10	2674
2–1	0.1820 ± 17	0.485 ± 4	12.2 ± 0.2	0.5811 ± 37	2.091	83	2300	0.69	2671
6–2*	0.1806 ± 6	0.461 ± 3	11.5 ± 0.1	0.1398 ± 9	0.574	528	5400	0.30	2658
1–2	0.1793 ± 16	0.498 ± 4	12.3 ± 0.1	0.5000 ± 33	1.854	90	4200	0.69	2646
15–1	0.1790 ± 7	0.489 ± 3	12.1 ± 0.1	0.2401 ± 11	0.870	337	7200	0.27	2643
16–1	0.1785 ± 11	0.507 ± 5	12.5 ± 0.2	0.1746 ± 16	0.631	261	4500	0.36	2639
7–1	0.1780 ± 16	0.492 ± 4	12.1 ± 0.1	0.5930 ± 36	2.172	85	3000	0.74	2634
4–1	0.1776 ± 36	0.501 ± 7	12.3 ± 0.3	0.0387 ± 67	0.193	59	800	2.01	2631
8–2*	0.1775 ± 10	0.490 ± 4	12.0 ± 0.1	0.3459 ± 19	1.205	179	4300	0.39	2630
13–1	0.1763 ± 23	0.500 ± 6	12.2 ± 0.2	0.4588 ± 49	1.677	110	1900	0.83	2618
9–1	0.1750 ± 28	0.482 ± 5	11.6 ± 0.2	0.3098 ± 56	1.170	48	940	1.70	2606
Inherited cores									
10–1	0.2130 ± 14	0.562 ± 5	16.5 ± 0.2	0.1321 ± 20	0.483	104	4200	0.45	2929
8–1	0.2129 ± 10	0.556 ± 4	16.3 ± 0.1	0.1352 ± 14	0.513	181	4000	0.40	2928
6–1	0.2115 ± 15	0.531 ± 4	15.5 ± 0.2	0.1441 ± 20	0.525	94	5500	0.57	2917
14–2	0.2111 ± 25	0.553 ± 6	16.1 ± 0.3	0.2124 ± 44	0.493	114	1100	1.52	2914
12–1	0.2108 ± 13	0.557 ± 4	16.2 ± 0.2	0.1527 ± 20	0.587	144	1900	0.88	2911
14–1	0.2107 ± 10	0.561 ± 4	16.3 ± 0.1	0.1835 ± 14	0.688	233	3700	0.45	2911
Composite core/rim									
6–4	0.1910 ± 7	0.527 ± 4	13.9 ± 0.1	0.0323 ± 7	0.131	309	11 300	0.16	2750
6–3	0.1824 ± 6	0.511 ± 5	12.8 ± 0.1	0.0054 ± 5	0.015	793	11 000	0.15	2675

*Denotes a magmatic rim on an older core.

Table 5 Compiled K–Ar analyses of selected minerals, Mt Narryer, Western Australia.

Sample No. GSWA	Mineral	K (%)		$^{40}Ar^*$ (10^{-10} mol/g)	$^{40}Ar^*/^{40}Ar$ (%)	Age (Ma ± 1σ)
71918	Hornblende	0.470	0.470	47.66	99.4	2607 ± 24
				47.87	99.2	2612 ± 24
71918	Biotite	2.58	2.55	136.1	99.0	1789 ± 16
71929	Hornblende	0.504	0.499	103.8	99.4	3664 ± 39
77239A	Plagioclase	0.167	0.167	10.20	97.5	1954 ± 18
77239A	Hornblende	0.716	0.715	82.58	99.5	2787 ± 25
77236	Plagioclase	0.249	0.247	16.65	99.0	2066 ± 19
77236	Hornblende	1.063	1.063	111.0	99.8	2645 ± 24
				113.0	99.7	2676 ± 24
71931	Biotite	7.37	7.42	47.84	99.9	2022 ± 22
60735	Biotite	7.30	7.32	42.24	99.8	1887 ± 17
60737	Biotite	6.52	6.50	34.21	99.6	1778 ± 16

The abundance of $^{40}K/K_{total}$ is 1.167×10^{-4} mol/mol.
The decay constants used for ^{40}K are: $\lambda_\beta = 4.962 \times 10^{-10}$/year, $\lambda_{(e+e')} = 0.581 \times 10^{-10}$/year.
$^{40}Ar^*/^{40}Ar$ is the percentage of radiogenic ^{40}Ar in the total measured ^{40}Ar.

same samples gave 1954 ± 36 and 2066 ± 38 Ma respectively.

With one exception, all these apparent ages are much younger than the known ages of the host rocks and of the supposed event of high-grade metamorphism at 3350 Ma, reflecting the protracted subsequent metamorphic history of the region. The apparent ages given by the hornblendes (2600–2800 Ma) consistently are higher than those obtained from biotite and plagioclase (1750–2100 Ma), implying that thermal perturbation of the less Ar-retentive minerals persisted well into the Proterozoic Era. One possibility for the exceptionally high K–Ar age of the hornblende in 71929 is that it contains locally derived excess argon evolved from the coexisting biotite during its partial recrystallization to chlorite. In order to clarify the K–Ar data, three $^{40}Ar/^{39}Ar$ stepheating experiments were carried out; two on hornblendes (samples 71918, 77236) and one on plagioclase (77236). Results are given in Table 6, and age spectra are illustrated in Fig. 8.

The hornblende from the para-amphibolite in the quartzite sequence (sample 71918) yielded ages in the initial steps of around 1000 Ma, increasing with some secondary structure to a maximum of 2780 Ma at high temperature (Fig. 8a). The K/Ca ratio, calculated from the measured $^{39}Ar_K/^{37}Ar$ ratio, was in the initial steps around 1.5, which may indicate the contribution of a phase other than hornblende ($K/Ca = 0.53 \times {}^{39}Ar_K/{}^{37}Ar$, as determined by repeated $^{40}Ar/^{39}Ar$ analysis of laboratory standard hornblende 77–600). The K/Ca ratios for the remainder of the age spectrum are typical of hornblende. The low ages and high K/Ca of the low temperature steps may thus have been caused by minor biotite contamination.

The hornblende from the Manfred Complex meta-anorthosite (sample 77236) yielded a regular age spectrum (Fig. 8b) with apparent ages rising from 2670 to 2720 Ma, and an integrated age of 2704 ± 14 Ma (2σ) over more than 90% of the gas release. The plagioclase from this sample produced a saddle-shaped age spectrum (Fig. 8c). In the first steps the apparent ages decrease from 4280 to 1340 Ma. Then in the middle part of the spectrum the ages increase to an apparent plateau at an integrated age of 1620 ± 12 Ma (2σ). In the final 28% of gas release, ages increase to values of *ca* 3540 Ma.

The hornblendes separated from the amphibolites in the metasedimentary belt and the anorthosites in the orthogneiss terrane each belong to the remnant high-grade mineral assemblages preserved in the respective host rocks, which in both cases are overprinted by greenschist facies chlorite–actinolite–epidote–calcite assemblages.

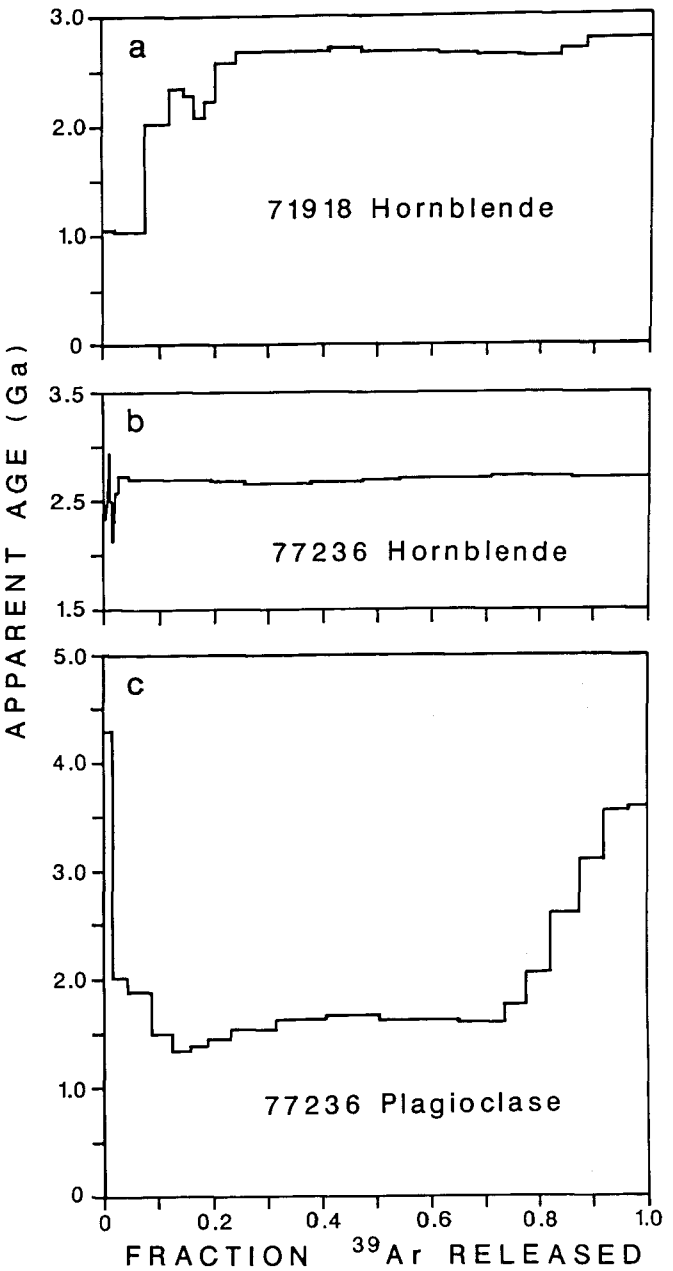

Fig. 8 $^{40}Ar/^{39}Ar$ age spectra of selected minerals.

Ideally, the $^{40}Ar/^{39}Ar$ age spectra should record for these samples the most recent time of cooling below the closure temperature of hornblende for Ar (*ca* 500°C; Harrison *et al* 1979). In this instance, only the anorthosite hornblendes yielded an uncomplicated age spectrum leading to a regular plateau at *ca* 2700 Ma. Although the amphibolite hornblendes gave similar ages in the high temperature steps, secondary irregularities obscure the ultimate age. Nevertheless, with the additional supporting evidence from the conventional K–Ar ages which for both samples are either comparable or slightly younger, it is concluded that around 2700 Ma both terranes were cooling after metamorphism to at least amphibolite facies grade.

Table 6 $^{40}Ar/^{39}Ar$ data, selected minerals, Mt Narryer region, Western Australia.

T (°C)	^{36}Ar (10^{-15} mol)	^{37}Ar (10^{-12} mol)	^{38}Ar (10^{-13} mol)	^{39}Ar (10^{-13} mol)	^{40}Ar (10^{-11} mol)	$^{40}Ar^*/^{40}Ar$ (%)	Age (Ma ± 1σ)
Sample 71918: hornblende (0.4058g, J = 0.01980, 180–250 μm)							
530	29.65	0.2598	0.5770	1.726	1.559	43.9	1047 ± 9
630	14.38	0.3021	1.748	6.686	3.047	86.1	1037 ± 4
720	6.469	0.1773	1.294	5.295	5.376	96.7	2026 ± 7
780	5.327	0.2101	1.204	2.791	3.935	96.0	2352 ± 8
830	6.159	0.3319	0.9706	2.319	3.153	94.3	2281 ± 8
870	5.517	0.4359	0.8274	1.993	2.339	93.2	2080 ± 7
910	6.324	0.9085	1.166	2.369	3.094	94.2	2231 ± 7
950	8.663	2.862	2.836	4.468	7.368	96.9	2579 ± 9
980	9.798	6.265	1.596	7.813	13.75	98.3	2692 ± 8
1000	11.89	10.49	7.856	12.23	21.30	98.8	2684 ± 8
1010	5.648	5.816	4.375	6.681	11.80	99.0	2717 ± 8
1020	6.671	7.181	5.260	8.124	14.10	99.0	2684 ± 8
1030	6.443	7.582	5.547	8.395	14.54	99.1	2682 ± 8
1040	5.837	7.969	5.478	8.626	14.79	99.3	2671 ± 8
1060	5.942	8.689	5.936	9.177	15.47	99.4	2648 ± 7
1080	5.213	8.625	5.545	8.788	14.61	99.5	2630 ± 7
1110	3.297	5.787	3.659	5.688	9.934	99.5	2630 ± 7
1140	4.342	8.092	5.403	7.998	14.75	99.6	2778 ± 8
Fusion	7.705	5.531	3.582	5.536	10.37	98.3	2780 ± 8
Σ	155.3	87.51	64.86	116.7	185.7	97.5	2547
Flux monitor (0.0787 g)							
	16.23	16.87	12.95	13.09	2.021	83.6	
Fusion (0.0434 g)							
	7.426	4.707	3.533	6.079	9.843	98.2	2574 ± 13
Sample 77236: hornblende (0.4725 g, J=0.01977, 100–180 μm)							
480	9.042	0.1721	0.2701	0.3352	0.9666	72.5	2957 ± 12
580	7.677	1.008	1.112	1.073	1.625	86.6	2317 ± 8
680	6.334	0.7556	0.6765	0.9687	2.135	91.5	2908 ± 9
730	5.119	0.2985	0.5573	0.8756	1.458	89.8	2484 ± 7
780	5.390	0.2372	0.4310	0.6984	0.9777	83.9	2169 ± 7
830	6.286	0.3696	0.5476	0.7641	1.056	82.7	2137 ± 8
870	4.703	0.4780	0.4442	0.5966	0.9446	85.7	2314 ± 8
910	6.456	1.037	0.7898	0.8898	1.603	88.7	2583 ± 7
950	8.849	3.587	7.141	5.679	10.30	97.8	2722 ± 8
980	6.134	5.293	17.47	14.15	24.72	99.4	2691 ± 7
1000	7.732	10.67	36.75	30.74	53.59	99.7	2692 ± 7
1010	6.261	6.231	20.30	17.61	30.59	99.6	2685 ± 7
1020	4.447	5.433	17.43	15.28	26.33	99.7	2675 ± 7
1030	4.766	6.438	21.24	18.51	31.84	99.7	2673 ± 7
1040	3.631	4.812	16.45	14.28	24.72	99.7	2683 ± 7
1050	2.772	4.394	15.21	13.21	22.93	99.8	2686 ± 7
1070	3.356	6.751	24.16	20.59	36.02	99.9	2699 ± 7
1090	8.844	16.47	62.69	50.90	90.29	99.9	2718 ± 7
1120	11.32	14.79	54.98	43.10	77.05	99.7	2727 ± 7
1160	21.31	8.150	27.95	21.98	39.08	99.8	2720 ± 7
Fusion	5.573	8.196	25.32	20.26	36.02	99.7	2720 ± 7
Σ	146.0	105.6	351.9	292.5	514.2	99.2	2698
Flux monitor (0.0655 g)							
	14.05	12.27	12.86	9.435	1.527	79.9	
Fusion (0.0226 g)							
	9.625	4.923	16.13	13.56	24.06	99.0	2706 ± 7

Table 6 Continued

T (°C)	^{36}Ar (10^{-15} mol)	^{37}Ar (10^{-12} mol)	^{38}Ar (10^{-13} mol)	^{39}Ar (10^{-13} mol)	^{40}Ar (10^{-11} mol)	$^{40}Ar^*/^{40}Ar$ (%)	Age (Ma ± 1σ)
Sample 77236: plagioclase (0.4915 g, J=0.02011, 100–180 μm)							
320	27.57	0.3946	0.6067	1.014	5.700	85.8	4281 ± 12
420	8.733	1.337	0.3684	1.764	2.031	87.9	2010 ± 7
500	8.806	3.168	0.6146	3.028	2.963	92.2	1875 ± 6
560	4.558	3.445	0.4133	2.762	1.867	94.4	1499 ± 6
600	3.000	3.191	0.3969	2.241	1.280	95.3	1343 ± 5
640	3.099	3.601	0.3796	2.344	1.377	95.7	1375 ± 5
680	3.348	4.853	0.5136	2.933	1.801	96.9	1431 ± 5
720	5.847	9.151	0.8407	5.704	3.849	97.6	1534 ± 5
760	5.512	8.758	1.031	6.468	4.725	98.2	1622 ± 6
800	6.087	9.138	0.8819	7.087	5.312	98.1	1648 ± 6
830	3.815	5.935	0.6695	4.338	3.128	98.1	1606 ± 5
860	4.854	6.391	0.8128	5.082	3.698	97.6	1611 ± 6
890	3.900	4.444	0.6016	3.734	2.709	97.2	1602 ± 6
920	3.895	3.289	0.4529	2.838	2.098	95.9	1607 ± 5
950	4.490	3.102	0.5115	2.660	2.267	95.4	1757 ± 6
990	6.343	3.819	0.6344	2.995	3.311	95.4	2064 ± 6
1040	10.63	6.470	0.8588	3.715	6.183	95.9	2610 ± 7
1100	10.89	7.883	0.8635	3.016	6.968	96.4	3097 ± 8
1180	14.90	13.23	0.9861	3.313	10.19	96.8	3553 ± 9
Fusion	20.40	16.15	0.9807	2.962	9.364	95.1	3585 ± 9
Σ	160.7	117.7	13.34	70.00	80.82	94.1	2139
Flux monitor (0.0821 g)							
	18.74	18.10	12.86	13.82	2.150	81.7	
Fusion (0.0853 g)							
	22.04	19.08	1.749	11.35	12.76	96.2	2099 ± 6

Quoted temperatures are the average of thermocouple measurement on the bottom of the sample crucible, and optical pyrometer measurement on the upper inside wall of the sample crucible. The difference between the two measurements typically was 150°C. The ^{39}Ar and ^{37}Ar concentrations are corrected for radioactive decay during irradiation and the period between irradiation and analysis. Laboratory standard hornblende 77-600 (K–Ar age 414.2 Ma) was used as a flux monitor. Absolute abundances were derived using the machine sensitivity (5.045×10^{-15} moles/mV), which was determined from regular measurement of standard minerals. Quoted uncertainties in apparent ages are the standard error, and include 0.5% uncertainty in parameter J. $\lambda = 5.543 \times 10^{-10}$/year.

The closure temperature for plagioclase is much lower (*ca* 200°C; Harrison *et al* 1979). The K–Ar analyses of biotites and plagioclase can be interpreted as indicating partial outgassing of radiogenic Ar during retrogression *ca* 1600 Ma, or else resetting by a more severe episode *ca* 2000 Ma followed by slow cooling.

DISCUSSION

In considering the isotopic integrity of an ancient detrital zircon population it must be remembered that zircons in ancient rocks presently exposed at the Earth's surface have invariably suffered some degree of recent Pb loss, particularly from those parts of crystals highly damaged by *in situ* decay of radioactive elements. Zircons which experienced an Archaean erosion cycle would likewise have suffered some Pb loss at the time of exposure. However, once liberated, zircons are mechanically sorted and modified in the surficial environment so that only pristine material is deposited quantitatively into mature quartz-rich sediments like the Mt Narryer quartzite. Exposed metamict components which are weak and brittle disintegrate during the early stages of erosion and transportation, whereas the surfaces of the remaining grains are smoothed off in a natural version of the air-abrasion technique for selection of concordant zircon.

Given the lack of shallow intra-grain discordance trajectories for low-U parts of detrital zircons and the preservation of near-concordant ages up to 4200 Ma, it is believed that the youngest near-concordant analyses of low-U zircons with igneous morph-

ologies in the Mt Narryer quartzite provide a firm older limit to the age of deposition. On this basis the sequence is constrained as being younger than *ca* 3280 Ma old. The Mt Dugel meta-pelite is similarly constrained to ≤3100 Ma old. These are maximum estimates for the time of sedimentation because appropriate source rocks would not necessarily have crystallized zircon up until the time of erosion, and not all contributing components necessarily are present in each sampled horizon. Hence, both sequences could be part of a single depositional system ≤3100 Ma in age. Additional evidence suggests that widespread deposition of quartz-rich sediments occurred in the Western Yilgarn at about that time. Composite fractions of detrital zircons in quartzites from the Jimperding Metamorphic Belt near Perth (Nieuwland & Compston 1981) yielded $^{207}Pb/^{206}Pb$ ages between 3250 and 3100 Ma, and the youngest concordant ages of zircons from the matrix of the Jack Hills chert pebble conglomerate, 60 km northeast of Mt Narryer, again are *ca* 3100 Ma (Compston & Pidgeon 1986). Clasts of chert and quartz–magnetite rock in conglomerates at Mt Narryer and at Jack Hills presumably were derived from older (though not necessarily much older) chemical sediments.

These results confirm that the metasediments at Mt Narryer and at Mt Dugel are younger than the adjacent orthogneisses, but also that, contrary to previous reports, the age of deposition post-dates the supposed high-grade metamorphism at 3350 Ma. Furthermore, because the sediments preserve amphibolite facies mineral assemblages, it follows that there must have been an episode of regional high-grade metamorphism younger than 3100 Ma. Either this was the only high-grade event in the regional history or, more likely, it followed earlier events which affected only the older orthogneiss terrane. There is no petrological evidence to suggest that the sediments were metamorphosed to high grades more than once. Geothermometry and geobarometry on biotite–garnet and garnet–cordierite pairs from quartzite samples 71919, 71923 and 71924 yielded temperature estimates in the range 420–720°C and pressures of 250–300 MPa (Wijbrans 1985). These values indicate substantial re-equilibration within the peak metamorphic assemblages, the highest temperatures being consistent with the amphibolite–granulite transition, and are considerably lower than a previously reported measurement of garnet–cordierite pairs in a sample of Mt Narryer quartzite which indicated 780°C and 510 MPa (Blight & Barley 1981).

An indication of the age of this metamorphism is provided by the hornblende $^{40}Ar/^{39}Ar$ age spectra which show that cooling below 500°C last took place at around 2700 Ma, some 300–400 Ma after sedimentation. Since the observed high-grade mineral assemblages suggest relatively low pressures it is unlikely that temperatures had been in excess of 500°C for an extended period, so the actual peak of metamorphism probably is little removed from this age. Irrespective of this argument, further evidence in support of a *ca* 2700 Ma age comes with the appearance of overgrowths of new zircon in the Mt Dugel meta-pelite at 2683 ± 8 Ma. It appears that by this time the meta-sediments and present-day basement gneisses had been brought together (given the similar hornblende age spectra), subsequently to be intruded by granite sheets *ca* 2650 Ma in age. The 2700 Ma event was thus a prograde event for the sediments but probably a retrograde event for the older orthogneisses for which there is evidence of earlier granulite facies metamorphism (Myers & Williams 1985).

The 3302 ± 6 Ma intrusion age indicated by isotopic compositions of the zircons from the porphyritic granite at Mt Narryer (MN26) is another key result of this study. This age is perfectly in agreement with equally precise crystallization ages of 3296 ± 4 Ma and 3295 ± 4 Ma (2σ) determined by ion probe for zircon overgrowths and whole grains interpreted as metamorphic in origin from two samples of the Meeberrie gneiss at Mt Narryer. One of these samples was taken from a locality only 1 km north of the granite exposure (sample 60735: Kinny *et al* 1988a), the other from the western side of the quartzite range (MN39: Kinny 1987). It is therefore proposed that growth of metamorphic zircon in the Meeberrie gneisses at Mt Narryer *ca* 3300 Ma took place during an episode of regional high-grade metamorphism which accompanied the widespread emplacement of granites at this time. Because the studied porphyritic granite possesses the D_2 flaser deformation fabric which Myers and Williams (1985) considered to have developed during granulite facies metamorphism, it is likely that 3300 Ma is the age of D_2 also.

The geological significance of the marginally older 3348 ± 43 Ma Rb–Sr isochron age (de Laeter *et al* 1981) is unclear but may reflect partial isotopic resetting during the proposed 3300 Ma metamorphism, bearing in mind that the individual analyses do not fit a least-squares regression to within experimental error. This implies that Sr isotopic homogenization was incomplete over the scale of sampling. Additional Rb–Sr analyses of Meeberrie gneiss samples from exposures southwest of Mt Narryer where it is intruded by the 2650 Ma granite sheets were poorly fitted to an isochron

with a younger apparent age of 3098 ± 132 Ma (de Laeter *et al* 1985). Fletcher *et al* (1988) emphasize the complexities of the Rb–Sr (and Pb/Pb) isotopic systematics of whole-rock and mineral systems in the region in terms of variable responses to the protracted history of metamorphic overprints. The intricacies of the various zircon Pb/U discordance patterns revealed by the ion probe can equally be attributed to the net superimposition of several ancient disturbances to the evolving chemical/isotopic domains within the individual grains.

The relationships between Sm–Nd model ages and zircon U–Pb ages for the Narryer region are illustrated graphically in Fig. 9. For the oldest identified components of the exposed crust (the Meeberrie gneisses and the Manfred Complex), the model ages are close to the interpreted crystallization ages of the igneous zircon populations, indicating that the Nd ages are consistent with derivation of these rocks from sources of approximately chondritic composition. However, for the younger granitic rocks for which data are available (the Dugel gneiss and the fine-grained granite sheets), the Nd ages are higher than the zircon ages. The increasing size of the age difference with each new addition to the terrane is interpreted as reflecting the increasing contribution of reworked older crust in the genesis of these rocks. This is supported by the presence of inherited pre-magmatic zircon cores in the igneous population from the younger granite MN38. The indicated age of these cores, 2919 ± 8 Ma, does not match with any identified zircon population age in the terrane at the present level of exposure, implying that they were assimilated from deeper crustal levels and that the present basement gneisses may have been thrust over younger units similar to those presently exposed 150 km to the south and southwest.

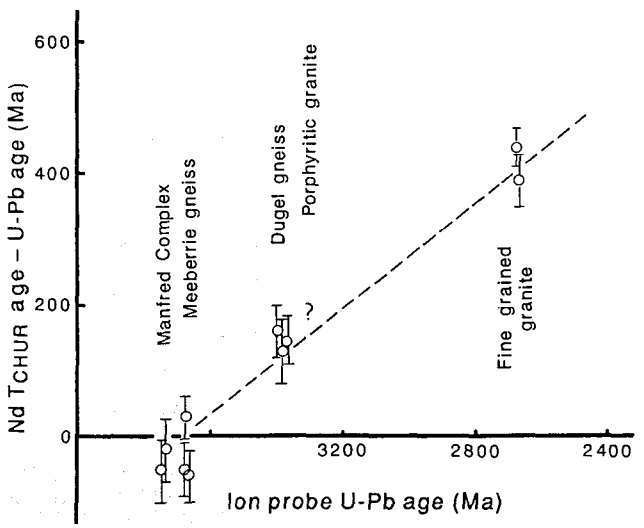

Fig. 9 Diagram showing the steady increase with time in the difference between the Sm–Nd model ages and U–Pb zircon ages of the major meta-igneous components of the Mt Narryer region. Sm–Nd ages are from de Laeter *et al* (1981, 1985) and Fletcher *et al* (1988). U–Pb ages are from Kinny *et al* (1988a), and from this paper. No Sm–Nd data presently exist for the 3300 Ma porphyritic granite.

PROVENANCE OF THE METASEDIMENTS

Well preserved graded and channel-bedding structures in the Mt Narryer quartzite sequence suggest a fluvio-deltaic depositional regime. The range of metasedimentary rock types present, from meta-pelite and amphibolite to orthoquartzite and meta-conglomerate, and the absence of volcanics suggest a stable littoral/shallow continental shelf lithofacies. A direct indication of source lithologies is provided by the composition of conglomerate clasts. Exposures of meta-conglomerate in the Mt Narryer sequence are restricted to quartz pebble conglomerates and poorly sorted polymict lenses comprised essentially of quartzite, vein-quartz and quartz–magnetite rock (meta-BIF) clasts (Myers & Williams 1985). This implies that older sedimentary rocks are present in the source regions, but probably exaggerates their importance because detritus from igneous rocks may be restricted to finer grain fractions. An additional suite of garnet-rich pebbles in the conglomerate lenses have in places been observed to be penetrated by other clasts, which indicates that they were semi-consolidated at the time of deposition. They probably represent fragments of channel bank muds.

Trace element chemical analyses of two quartz-rich meta-pelites from the Mt Narryer quartzite sequence and for the Mt Dugel meta-pelite (MN45) (Taylor *et al* 1986) indicate that each is enriched in the light rare earth elements and each possesses a pronounced negative Eu anomaly. According to Taylor and McLennan (1985) such REE abundance patterns in sediments are inherited from K-rich granitic source rocks derived in turn from intracrustal partial melting episodes during which Eu is fractionated into restitic plagioclase. Further, among the accessory phases in one of the Mt Narryer samples, Taylor *et al* (1986) noted the presence of detrital thortveitite, a rare scandium silicate mineral which is known only from pegmatites associated with alkalic granites (e.g. Neumann 1961; Sakurai *et al* 1962).

These observations support a model of deposition *ca* 3100 Ma at the margin of an evolved

block of Archaean continental crust, of which potassic granites (*s.l.*) were an important component. Rock fragments preserved in conglomerate layers prove that older sediments also were present. Additionally, a contribution from mafic lithologies is indicated by high Cr and Ni contents of MN45 (Taylor *et al* 1986) and by the abundance of detrital chromite in the Jack Hills conglomerate. The evidence from detrital zircons indicates that a portion of this crust was formed between 4270 Ma and 4100 Ma (Froude *et al* 1983; Compston & Pidgeon 1986) and remained intact until erosion and sedimentation 1000 Ma later. The 3% abundance of these zircons in the matrix of the Jack Hills conglomerate (R. Maas pers. comm. 1989) suggests that they were derived from a voluminous, fertile source of zircon by the first cycle of erosion and sedimentation. It is concluded that this source was stable felsic crust which had evidently survived unscathed the intense meteorite bombardment in the Earth's early history but which was later reworked by tectonic uplift and erosional processes akin to those occurring at present at active continental margins or rifts. Therefore, intact remnants of this crust may still exist in the region. The K-rich felsic gneisses, granites and anorthositic rocks presently juxtaposed to the Mt Narryer quartzite are candidates for the sources of some of the younger detrital zircons, although, as pointed out by Kinny *et al* (1988a), the indicated crystallization ages of these components do not match particular peaks in the age spectrum of the detrital zircons. Other source terranes may have been more important contributors.

The oldest known components of other Early Archaean terranes are no older than *ca* 3900 Ma, that is those in Enderby Land, Eastern Antarctica (Black *et al* 1986) and the Godthåbsfjord region of southern West Greenland (Kinny *et al* 1988b). The unique presence of 4100–4200 Ma-old detrital zircons in mid-Archaean sediments of the Narryer Gneiss Complex, the fact that these sediments contain REE abundance patterns usually restricted to post-Archaean sediments, and the presence of extensive Early Archaean gneisses derived from potassic granites all support the idea that stable continental crust evolved in this region at an earlier stage than perhaps any other preserved exposure of the Earth's earliest crust.

CONCLUSIONS

Table 7 summarizes the revised geological history of the Mt Narryer region derived from the above data. Of principal significance is the firm older constraint of 3280 Ma now applied to the deposition age of the Mt Narryer sequence, which when correlated with the Mt Dugel and Jack Hills sequences may be further restricted to *ca* 3100 Ma. The history of deformation and metamorphism of the sediments must therefore be fitted to a younger time scale and not correlated as previously with earlier events affecting the presently juxtaposed orthogneiss terrane. Prograde amphibolite facies metamorphism of the sediments evidently culminated around 2700 Ma, prior to intrusion of the fine grained granite sheets around 2650 Ma. By the end of the Archaean the present tectonic framework had been established, and the entire region underwent patchy retrogression under greenschist facies in the mid-Proterozoic.

Another key result is the 3300 Ma age for the porphyritic granite northeast of Mt Narryer, which is perfectly in agreement with the age of metamorphic zircon overgrowths in the Meeberrie gneiss which it intrudes. This provides an older limit for the age of D_2 deformation considered by Myers and Williams (1985) to be associated with granulite facies metamorphism, and which has previously been associated with a slightly older Rb–Sr isochron age. The intrusion of 3300 Ma old granites may be

Table 7 Revised geological history of the Mt Narryer region. Ages in Ma.

2000–1600	Greenschist facies retrogression Recrystallization of young granites
2650	Fine grained granite intrusions
2700	Zircon overgrowths in pelitic paragneiss Amphibolite facies metamorphism Movement on shear zones to present configuration
?	Syncline folding of sediments D_3 (refolding of orthogneisses)
2920	Basement protolith later incorporated into 2650 Ma granites
3100–?	Deposition of sediments
3300	Porphyritic granite intrusion Zircon overgrowths in gneisses D_2 (flaser fabric — orthogneisses)[3]
3380	Dugel gneiss protolith[3]
?	D_1 (gneissose banding)
3680	Meeberrie gneiss protolith[3]
3730	Manfred layered igneous complex[3]
4270–4100	Early crust[1, 2]

Additional sources: [1]Froude *et al* 1983; [2]Compston & Pidgeon 1986; [3]Kinny *et al* 1988a.

synchronous with D_2 and the associated high-grade metamorphism.

ACKNOWLEDGEMENTS

The former Director of the Geological Survey of Western Australia, Dr A. F. Trendall, is thanked for logistic support of fieldwork, and Drs I. McDougall and A. P. Nutman for their comments on preliminary drafts of this manuscript.

REFERENCES

BLACK L. P., WILLIAMS I. S. & COMPSTON W. 1986. Four zircon ages from one rock: The history of a 3930 Ma-old granulite from Mount Sones, Enderby Land, Antarctica. *Contributions to Mineralogy and Petrology* **94**, 427–437.

BLIGHT D. F. & BARLEY M. E. 1981. Estimated pressure and temperature conditions from some Western Australian Precambrian metamorphic terrains. *Geological Survey of Western Australia, Annual Report* **1980**, 67–72.

COMPSTON W., WILLIAMS I. S. & MEYER C. 1984. U–Pb geochronology of zircons from Lunar breccia 73217 using a sensitive high mass-resolution ion microprobe. *Journal of Geophysical Research* **89**, Supplement, B525–534.

COMPSTON W. & PIDGEON R. T. 1986. Jack Hills, evidence of more very old detrital zircons in Western Australia. *Nature* **321**, 766–769.

CUMMING G. L. & RICHARDS J. R. 1975. Ore lead isotope ratios in a continuously changing earth. *Earth and Planetary Science Letters* **28**, 155–171.

DE LAETER J. R., FLETCHER I. R., ROSMAN K. J. R., WILLIAMS I. R., GEE R. D. & LIBBY W. G. 1981. Early Archaean gneisses from the Yilgarn Block, Western Australia. *Nature* **292**, 322–324.

DE LAETER J. R., FLETCHER I. R., BICKLE M. J., MYERS J. S., LIBBY W. G. & WILLIAMS I. R. 1985. Rb–Sr, Sm–Nd and Pb–Pb geochronology of ancient gneisses from Mt Narryer, Western Australia. *Australian Journal of Earth Sciences* **32**, 349–358.

FLETCHER I. R., ROSMAN K. J. R. & LIBBY W. G. 1988. Sm–Nd, Pb–Pb and Rb–Sr geochronology of the Manfred Complex, Mount Narryer, Western Australia. *Precambrian Research* **38**, 343–354.

FROUDE D. O., IRELAND T. R., KINNY P. D. *et al* 1983. Ion microprobe identification of 4100–4200 Myr-old terrestrial zircons. *Nature* **304**, 616–618.

GEE R. D., MYERS J. S. & TRENDALL A. F. 1986. Relation between Archaean high-grade gneiss and granite–greenstone terrain in Western Australia. *Precambrian Research* **33**, 87–102.

HARRISON T. M., ARMSTRONG R. L., NAESER C. W. & HARAKAL J. E. 1979. Geochronology and thermal history of the Coast Plutonic Complex, near Prince Rupert, BC. *Canadian Journal of Earth Sciences* **16**, 400–410.

KINNY P. D. 1987. An ion microprobe study of uranium–lead and hafnium isotopes in natural zircon. PhD thesis, Australian National University (unpubl.).

KINNY P. D., WILLIAMS I. S., FROUDE D. O., IRELAND T. R. & COMPSTON W. 1988a. Early Archaean zircon ages from orthogneisses and anorthosites at Mount Narryer, Western Australia. *Precambrian Research* **38**, 325–341.

KINNY P. D., COMPSTON W. & MCGREGOR V. R. 1988b. The early Archaean crustal history of West Greenland as recorded by detrital zircons. *In* Ashwal L. D. ed. *Workshop on the Growth of Continental Crust*, pp. 79–81. LPI Technical Report 88-02, Lunar and Planetary Institute, Houston.

MCDOUGALL I. 1974. The $^{40}Ar/^{39}Ar$ method of K–Ar age determination of rocks using HIFAR reactor. *Atomic Energy in Australia* **17**, 3–12.

MCDOUGALL I. & ROKSANDIC Z. 1974. Total fusion $^{40}Ar/^{39}Ar$ ages using HIFAR reactor. *Journal of the Geological Society of Australia* **21**, 81–89.

MCDOUGALL I. & SCHMINCKE H. 1977. Geochronology of Gran Canaria, Canary Islands. *Bulletin of Volcanology* **40**, 57–77.

MYERS J. S. 1988a. Early Archaean Narryer Gneiss Complex, Yilgarn craton, Western Australia. *Precambrian Research* **38**, 297–307.

MYERS J. S. 1988b. Oldest known terrestrial anorthosite at Mount Narryer, Western Australia. *Precambrian Research* **38**, 309–323.

MYERS J. S. & WILLIAMS I. R. 1985. Early Precambrian crustal evolution at Mount Narryer, Western Australia. *Precambrian Research* **27**, 153–163.

NEUMANN H. 1961. The scandium content of some Norwegian minerals and the formation of thortveitite, a reconnaissance survey. *Norsk Geologisk Tidsskrift* **41**, 197–210.

NIEUWLAND D. A. & COMPSTON W. 1981. Crustal evolution in the Yilgarn Block near Perth, Western Australia. *Geological Society of Australia, Special Publication* **7**, 159–171.

SAKURAI K., NAGASHIMA K. & KATO A. 1962. Thortveitite from Kobe, Omiya, Kyoto, Japan. *Bulletin of the Chemical Society of Japan* **35**, 1776–1779.

SCHÄRER U. & ALLÈGRE C. J. 1985. Determination of the age of the Australian Continent by single-grain zircon analysis of Mt Narryer metaquartzite. *Nature* **315**, 52–55.

STEIGER R. H. & JÄGER E. 1977. Subcommission on Geochronology: Convention on the use of decay constants in geo- and cosmochronology. *Earth and Planetary Science Letters* **36**, 359–362.

TAYLOR S. R. & MCLENNAN S. M. 1985. *The Continental Crust: Its Composition and Evolution.* Blackwell Scientific Publications, Oxford.

TAYLOR S. R., RUDNICK R. L., MCLENNAN S. M. & ERIKSSON K. A. 1986. Rare earth element patterns in Archean high-grade metasediments and their tectonic significance. *Geochimica et Cosmochimica Acta* **50**, 2267–2279.

TETLEY N. W., MCDOUGALL I. & HEYDEGGER H. R. 1980. Thermal neutron interferences in the $^{40}Ar/^{39}Ar$ dating technique. *Journal of Geophysical Research* **85**, 7201–7205.

WIJBRANS J. R. 1985. Geochronology of metamorphic terrains by the $^{40}Ar/^{39}Ar$ age spectrum method. PhD thesis, Australian National University (unpubl.).

WILLIAMS I. S. & CLAESSON S. 1987. Isotopic evidence for the Precambrian provenance and Caledonian metamorphism of high grade paragneisses from the Seve Nappes, Scandinavian Caledonides: II. Ion microprobe zircon U–Th–Pb. *Contributions to Mineralogy and Petrology* **97**, 205–217.

(*Received* 12 *April* 1989; *accepted* 3 *July* 1989)